Robust Distal Tip Cell Pathfinding in the Face of Temperature Stress Is Ensured by Two Conserved microRNAS in Caenorhabditis elegans

Robust Distal Tip Cell Pathfinding in the Face of Temperature Stress Is Ensured by Two Conserved microRNAS in *Caenorhabditis elegans*

Samantha L. Burke,* Molly Hammell,† and Victor Ambros*,[1]
*Program in Molecular Medicine, University of Massachusetts Medical School, Worcester, Massachusetts 01605, and †Watson School of Biological Sciences, Cold Spring Harbor Laboratory, Cold Spring Harbor, New York 11724

ABSTRACT Biological robustness, the ability of an organism to maintain a steady-state output as genetic or environmental inputs change, is critical for proper development. MicroRNAs have been implicated in biological robustness mechanisms through their post-transcriptional regulation of genes and gene networks. Previous research has illustrated examples of microRNAs promoting robustness as part of feedback loops and genetic switches and by buffering noisy gene expression resulting from environmental and/or internal changes. Here we show that the evolutionarily conserved microRNAs *mir-34* and *mir-83* (homolog of mammalian *mir-29*) contribute to the robust migration pattern of the distal tip cells in *Caenorhabditis elegans* by specifically protecting against stress from temperature changes. Furthermore, our results indicate that *mir-34* and *mir-83* may modulate the integrin signaling involved in distal tip cell migration by potentially targeting the GTPase *cdc-42* and the beta-integrin *pat-3*. Our findings suggest a role for *mir-34* and *mir-83* in integrin-controlled cell migrations that may be conserved through higher organisms. They also provide yet another example of microRNA-based developmental robustness in response to a specific environmental stress, rapid temperature fluctuations.

KEYWORDS *mir-34*; *mir-83*; *mir-29*; distal tip cell migrations; robustness

THE ability of a living system to maintain a steady-state output in the face of environmental and physiological stresses is referred to as biological robustness (Kitano 2004). Organisms must be able to compensate for adverse changes in gene expression caused by environmental stresses and internal gene expression noise if development is to proceed unchanged. The nematode *Caenorhabditis elegans* is a useful model for studying such robustness. *C. elegans* development has been mapped to a cell-by-cell level, such that we know exactly when cell divisions occur and what the fate of each cell is (Sulston 1976; Sulston and Horvitz 1977; Kimble and Hirsh 1979; Sulston *et al.* 1983). There is also extensive research on the worm's responses to stress, including stress-induced alternative larval developmental choices such as stage-specific diapause (Baugh and Sternberg 2006; Fukuyama *et al.* 2006; Ruaud and Bessereau 2006; Schindler *et al.* 2014) and proceeding to the dauer larvae stage, an alternative third larval stage that allows *C. elegans* to lengthen their lifespan and survive food deprivation or heat stress (Cassada and Russell 1975; Liu *et al.* 1995).

MicroRNAs (miRNAs) are single-stranded RNAs of ~22 nucleotides that negatively regulate the translation of their target messenger RNAs (mRNAs) by binding to their 3′ untranslated region (3′ UTR) as part of a protein–RNA complex called the miRNA-induced silencing complex (miRISC). Target recognition is determined by the miRNA's seed sequence, nucleotides two through seven (reviewed in Ambros 2004; Bartel 2004). miRNAs with the same seed sequence can presumably regulate the same target mRNAs and are grouped together within a miRNA family (reviewed in Bartel 2009). In addition to being regulated by multiple members of a miRNA family, an mRNA can be cotargeted by multiple distinct miRNAs families, if it contains the corresponding distinct seed-complementary sites. Such interfamily and intrafamily cotargeting is considered one reason why most single miRNA gene deletion mutants in *C. elegans* do not display apparent phenotypes; although one negative

doi: 10.1534/genetics.115.179184
Manuscript received March 12, 2015; accepted for publication June 10, 2015; published Early Online June 15, 2015.
Available freely online through the author-supported open access option.
Supporting information is available online at www.genetics.org/lookup/suppl/doi:10.1534/genetics.115.179184/-/DC1.
[1]Corresponding author: Program in Molecular Medicine, Biotech Two, Suite 306, 373 Plantation St., University of Massachusetts Medical School, Worcester, MA 01605. E-mail: victor.ambros@umassmed.edu

regulator is deleted, the target mRNAs in question remain under the regulation of additional, functionally redundant miRNAs (Miska *et al.* 2007; Alvarez-Saavedra and Horvitz 2010). Findings reported by the Abbott lab exemplified this phenomenon (Brenner *et al.* 2010). They screened for developmental phenotypes resulting from miRNA deletions in genetically sensitized backgrounds, in which the miRNA-specific argonaute protein *alg-1* was no longer functional. In the *alg-1* mutant background, overall miRNA production is partially compromised, such that the additional deletion of an otherwise redundant single miRNA can result in target deregulation and visible phenotypes.

In their study, the Abbott lab members identified six miRNAs involved in gonad morphogenesis (Brenner *et al.* 2010), a normally robust developmental process that is dependent on the migration of two distal tip cells (DTCs) (reviewed in Wong and Schwarzbauer 2012). One of these miRNAs included *mir-83*, a miRNA that is highly conserved in animals, including mammals (known as *mir-29*, Supporting Information, Figure S1) (Lagos-Quintana *et al.* 2001, 2002; Lau 2001; Mourelatos *et al.* 2002; Dostie *et al.* 2003; Lim *et al.* 2003; Lim 2003; Michael *et al.* 2003; Suh *et al.* 2004; Poy *et al.* 2004; Landgraf *et al.* 2007; Lui *et al.* 2007). Mammalian *mir-29* has been previously implicated in regulating cellular proliferation, differentiation, apoptosis, and the extracellular matrix (reviewed in Boominathan 2010; Kriegel *et al.* 2012). To better understand how *mir-83* functions, we set out to determine its mRNA targets and miRNA coregulators in *C. elegans*. Using mirWIP (Hammell *et al.* 2008), we noticed an overlap between the predicted mRNA targets for *mir-83* and *mir-34*, another miRNA that is conserved between nematodes and mammals (Figure S1, Table S1) (Lau 2001; Ambros *et al.* 2003; Grad *et al.* 2003; Houbaviy *et al.* 2003; Lim *et al.* 2003; Lim 2003; Landgraf *et al.* 2007). *mir-34* has been shown to have tumor suppressor activity in mammalian systems. There, its transcription is activated by p53 and it functions to reinforce p53 negative regulation (reviewed in He *et al.* 2007; Yamakuchi and Lowenstein 2009; Hermeking 2009; Rokavec *et al.* 2014).

To further understand the roles of *mir-83* and *mir-34*, we tested for genetic redundancy by creating the double mutant and looking at developmental phenotypes. We also identified potential targets of *mir-34* and *mir-83* by tests of genetic suppression. *mir-83(n4638)*; *mir-34(gk437)* double mutants display a defect in gonad morphogenesis. In addition, this defect reflects a loss of developmental robustness; the *mir-83(n4638)*; *mir-34(gk437)* phenotype is significantly enhanced in response to temperature changes but not by other environmental stresses that we tested. Based on our results, we conclude that *mir-34* and *mir-83* function together to help create or maintain robust function of the genetic network controlling gonad morphogenesis, such that the development of this important organ is protected from the temperature changes *C. elegans* may encounter, either the rapid oscillations tested here or subtler changes experienced in the wild. Furthermore, we observed that *mir-83(n4638)*; *mir-34(gk437)* mutants have a decreased lifespan and decreased fecundity, suggesting that the loss of these two miRNAs has repercussions for the biological fitness of the animals.

Materials and Methods

C. elegans strains

The *C. elegans* Bristol N2 strain was used as wild type in the study (Brenner 1974). Additional strains are listed in Table S2. Both the *n4638* and *gk437* alleles were backcrossed to N2 four times upon receipt. The VT2595 strain was used as the *mir-83(n4638)*; *mir-34(gk437)* double mutant except when VT3289 is explicitly discussed in Figure 2C.

C. elegans maintenance

Strains were maintained using standard procedures on nematode growth media (NGM) plates seeded with *Escherichia coli* strain HB101 (Brenner 1974), unless explicitly stated as being raised on OP50. Strains were raised at 20° unless otherwise stated when temperature was oscillated.

Sequence alignments, target prediction, and statistical significance

MicroRNA sequences were supplied by miRBase (Lagos-Quintana *et al.* 2001; Lau 2001; Lagos-Quintana *et al.* 2002; Mourelatos *et al.* 2002; Ambros *et al.* 2003; Aravin *et al.* 2003; Dostie *et al.* 2003; Grad *et al.* 2003; Houbaviy *et al.* 2003; Lim *et al.* 2003; Lim 2003; Michael *et al.* 2003; Sempere *et al.* 2003; Griffiths-Jones 2004; Poy *et al.* 2004; Suh *et al.* 2004; Griffiths-Jones *et al.* 2006, 2008; Landgraf *et al.* 2007; Lui *et al.* 2007; Kozomara and Griffiths-Jones 2011, 2014) and aligned by eye. Predicted targets were identified using mirWIP (Hammell *et al.* 2008). Throughout the manuscript, three significance asterisks (***) are used for a *P*-value of $\leq$0.005, two (**) for a *P*-value $>$0.005 and $\leq$0.01, and one (*) for a *P*-value $>$0.01 and $\leq$0.05.

Migration defective phenotype scoring

Hypochlorite treatment (Stiernagle 2006) was used to isolate embryos. Where noted, synchronized populations were created by allowing embryos to hatch in M9 buffer for ~24 hr (Johnson *et al.* 1984). Embryos or starved L1's were then plated on HB101-seeded NGM plates and raised to adulthood in the temperature scheme noted. Day one adults were paralyzed in 100 mM levamisole, mounted on 2% agarose pads, and scored using a Zeiss Axioskop differential interference contrast (DIC) microscope and a $\times$63 objective. A two-proportion *z*-test was used to determine significant differences between counts except where triplicates are presented. In such cases mean values were compared using an unpaired *t*-test performed by PRISM.

Temperature oscillations

Temperature oscillations were performed using modified MJ Research Programable Thermocyclers. First, the Thermocyclers'

lids were removed. Next, a 0.25-inch-thick aluminum plate was attached to the heat block using silicone-based thermal conductive grease. Original lids were replaced by insulating covers constructed out of styrofoam. HB101-seeded NGM plates containing worms were placed inside the modified device, in contact with the aluminum plate. To assess the thermal dynamics of the system, a thermometer was embedded in an NGM plate and the temperature of the agar was monitored during programmed temperature cycles. We observed that the temperature of NGM plates did cycle in accordance with the Thermocycler program, although not as quickly as the heat block itself; we observed an ~15- to 30-sec delay as the NGM cools or heats. Stated temperature cycles refer to the program run by the Thermocycler.

Electron microscopy

N2 and *mir-83(n4638)* IV; *mir-34(gk437)* X embryos were isolated using hypochlorite treatment, hatched in M9 buffer for ~24 hr and plated as synchronized L1's on HB101-seeded NGM plates. Worms were raised with temperature oscillations: 20° for 16 hr (15° for 15 min, 25° for 15 min, repeat three additional times), 20° until young adulthood. Worms were fixed and prepared for electron microscopy as previously described (Irazoqui *et al.* 2010) except they were cut below the pharynx rather than in half to preserve gonad morphology. Electron microscopy work was performed by the University of Massachusetts Medical School Electron Microscopy Core Facility.

Cloning and transgenics

Constructs were created using Life Technologies Gateway Cloning. Except where otherwise stated, gene fragments were first amplified from N2 genomic DNA using the primers listed in Table S3. PCR was next used to add the proper *att* sequences such that fragments could be moved into the appropriate Gateway DONR vector, as described in the Gateway Protocol. For the *mir-34* promoter, the 5-kb promoter was digested from a separate plasmid and ligated to a modified 476p5Emcs (a gift from Nathan Lawson's lab, modified to remove unnecessary *Sal*I cut sites) to add the necessary *att* sites. For mutated 3′ UTRs, DNA fragments of the desired sequence were created *de novo* by GeneWiz. The constructed DONR vectors, along with two commercially available vectors, were then used for transgene construction as described in the Gateway Protocol (Table S4). The destination vectors were developed for the Mos1-mediated single-copy insertion technique (Frøkjaer-Jensen *et al.* 2008), which was used to generate transgenic strains (Table S2). Multicopy arrays were generated for *cdc-42* and *pat-3* GFP/mCherry reporters. *mir-83(n4638)* IV; *mir-34(gk437)* X males were first crossed to EG6701 to create a *unc-119(ed3)* III; *mir-83(n4638)* IV; *mir-34(gk437)* X strain (VT3087). VT3087 was subsequently injected with a mix of pBluescript SK+ (30 ng/μl), pIF9 (15 ng/μl), pCFJ150 (30 ng/μl), pCFJ210 (30 ng/μl), and either pSLB054 (3 ng/μl) and pSLB056 (3 ng/μl) or pSLB071 (3 ng/μl) and pSLB075 (3 ng/μl). Array maEx246 was generated from the pSLB054- and pSLB056-containing injection mix, while array maEx247 was made from the pSLB071 and pSLB075 mix. The array carrying strains, VT3118 (for maEx246) and VT3145 (for maEx247), were crossed to N2 males to cross out the *mir-83(n4638)* and *mir-34(gk437)* deletions, generating strains VT3136 and VT3178, respectively.

RNAi

RNA-mediated interference (RNAi) was performed by raising animals on dsRNA-producing *E. coli* as described in Kamath *et al.* (2001). Synchronized L1's were placed on *cdc-42* RNAi food, *pat-3* RNAi food, or empty vector control food, and raised to young adulthood with the temperature scheme stated. Animals were scored as previously described.

Target reporter scoring

Hypochlorite treatment was used to isolate embryos, which were hatch in M9 to generate synchronized L1's. Worms were plated on HB101-seeded NGM plates and raised with temperature oscillations: 20° for 16 hr (15° for 15 min, 25° for 15 min, repeat three additional times), 20° until time of scoring. L1 animals were scored starting 18 hr postplating, immediately following temperature oscillations. L3 animals were scored starting 43 hr postplating, shortly after the molt from L2 to L3. Adults were scored starting 67 hr postplating, after egg laying had commenced.

Worms were suspended in 100 mM levamisole, mounted on 2% agarose pads, and scored using a Leica TCS SPE confocal microscope. For *cdc-42* reporters, DTCs were first identified in the DIC setting by eye using the ×63 objective. The confocal microscopy setting was subsequently used for imaging and quantifying the mean value florescence of each channel for a DTC using the Leica LAS AF software. For *pat-3* reporters, the ×10 objective was used to observe whole animals. A 30-step *z*-series was taken per worm. The Leica AF software was used to quantify mean value fluorescence for each channel using the *z*-stack maximum projection. Datasets were compared using an unpaired *t*-test performed by PRISM.

Brood size counts

N2 and *mir-83(n4638)* IV; *mir-34(gk437)* X embryos were isolated using hypochlorite treatment and left in M9 buffer for ~24 hr to hatch. Arrested L1's were then plated on HB101-seeded NGM plates and either raised at 20° continuously or with temperature oscillations from hour 16 to hour 18 postplating [labeled "cycled"—20° for 16 hr (15° for 15 min, 25° for 15 min, repeat three additional times), 20° until death]. Worms were individually plated as L4's, and the number of live offspring were counted from the start of egg laying until its end. Mean values were compared using an unpaired *t*-test performed by PRISM.

Mating assays

N2 and *mir-83(n4638)* IV; *mir-34(gk437)* X embryos were isolated using hypochlorite treatment and left in M9 buffer

for ~24 hr to hatch. Arrested L1's were then plated on HB101-seeded NGM plates and either raised at 20° continuously or with temperature oscillations from hour 16 to hour 18 postplating [labeled "cycled"—20° for 16 hr (15° for 15 min, 25° for 15 min, repeat three additional times), 20° until death]. Once they reached adulthood, hermaphrodites were transferred daily away from progeny until the ability to lay eggs was exhausted (day four of adulthood). Each hermaphrodite was then moved to an individual plate, to which four 1-day-old adult N2 males were added. Animals were allowed to mate for 3 days, at which point the males were removed. The total number of offspring that hatched were counted for each hermaphrodite from the start of the assay until its death.

Lifespan assays

Survival assays were performed similarly to previously described (Kenyon *et al.* 1993). N2 and *mir-83(n4638)* IV; *mir-34(gk437)* X embryos were isolated using hypochlorite treatment and left in M9 buffer for ~24 hr to hatch. Arrested L1's were then plated on HB101-seeded NGM plates and either raised at 20° continuously or with temperature oscillations from hour 16 to hour 18 postplating [labeled "cycled"—20° for 16 hr (15° for 15 min, 25° for 15 min, repeat three additional times), 20° until death]. To track survival, 100 worms per replicate and three replicated per condition were moved to a new HB101-seeded NGM plate as L4's. Worms were transferred to a new plate daily during the course of the assay to avoid overcrowding from the offspring. Worms were scored as alive or dead based on reaction to a gentle nose prod using a standard worm pick. Animals were tracked until their death. Any worms that died as a consequence of crawling up the side of the plate were removed from the assay. Replicates were used to calculate percent survival and the standard deviation for each day. Mean values for individual days were compared using a two sample *t*-test for means.

Additional stresses

Animals was raised on NGM plates containing 0.03% sodium arsenite to induce oxidative stress (Sahu *et al.* 2013). Incubation in 1% SDS for 30 min was used to isolate dauer animals from starved plates (Stiernagle 2006). Animals were raised on *Pseudomonas auruginosa* PA14 plates as previously described (Powell and Ausubel 2008).

Results

Improper distal tip cell migration paths in mir-83(n4638); mir-34(gk437) mutants

The shape of the *C. elegans* adult hermaphrodite gonad is determined by the migration of two DTCs, somatic gonadal cells at the tip of each gonad arm that drag the proliferative portion of the gonad with them as they migrate during the second through fourth larval stages of hermaphrodite development (Kimble and Hirsh 1979; Kimble and White 1981; Hedgecock *et al.* 1987). Both DTCs are born near the midbody during the first larval stage and begin to migrate along the ventral body wall muscles toward the head and tail during the second larval stage, referred to as phase 1 of migration (Hirsh *et al.* 1976; Kimble and Hirsh 1979; Kimble and White 1981). During phase 2, DTCs first turn dorsally to migrate from the ventral to the dorsal body wall muscle, crossing the hypodermis in the process (Hedgecock *et al.* 1987). A second turn is required to continue migration along the dorsal body wall muscles and return to the midbody (phase 3), creating two *U*-shaped gonad arms (Figure 1A) (Hirsh *et al.* 1976; Kimble and Hirsh 1979; Hedgecock *et al.* 1987). The final shape of the gonad arms can be used to deduce the path taken by each DTC. In a fraction of *mir-83(n4638)*; *mir-34(gk437)* mutants (26% at 20°, quantified in Figure 2), anterior and posterior gonad arms appear displaced at various positions, improperly crossing the dorsal/ventral axis (Figure 1B). These misplaced gonad arms suggest DTCs wandered from the proper path during phase 1 and/or phase 3 of migration and often migrated too far and past the developing vulva. The penetrance of this overextension phenotype was highly variable and overextension was observed to occur either with or without wandering during phase 1 and/or phase 3. Unlike some classes of *C. elegans* migration mutants, DTCs in *mir-83(n4638)*; *mir-34(gk437)* mutants execute both their first (dorsal) and second (anterior/posterior) turns at the proper positions in the animals and at the proper times in development. The migration defect of these mutants therefore reflects a defect in the precise pathfinding of the DTCs as they migrate longitudinally along the ventral or dorsal muscle. To score this phenotype we categorized gonad arms as either migration defective or normal. Gonad arms were categorized as migration defective if their abnormal shape indicated that the DTC had improperly crossed the dorsal/ventral axis during its migration, or that the DTC migrated completely past the vulva before stopping. Previously published findings indicated a low level of migration defects in the N2 strain (Peters *et al.* 2013). These included such phenotypes as DTCs stopping slightly short of the vulva and a slight ventralward "dip" of the DTCs when migration ceases. We observed such phenotypes as well, but due to their occurrence in N2 we classified such cases as within normal variation and did not score them as migration defects. It is also important to note that in the previously mentioned study (Peters *et al.* 2013), strains were raised at 23° rather than 20°.

DTC wandering results in displaced gonad arms, which is reflected in a reorganization of the internal organs. To visualize this reorganization in *mir-83(n4638)*; *mir-34(gk437)* mutants, we performed electron microscopy on cross-sections of adult worms. We first collected ~20 *mir-83(n4638)*; *mir-34(gk437)* worms whose anterior arm displayed a migration defect. These mutants and age-matched N2's were fixed and processed for electron microscopy. As previously described, in N2 worms the intestine spans the dorsal/ventral axis (Figure 1C) (Hall and Altun 2008). The

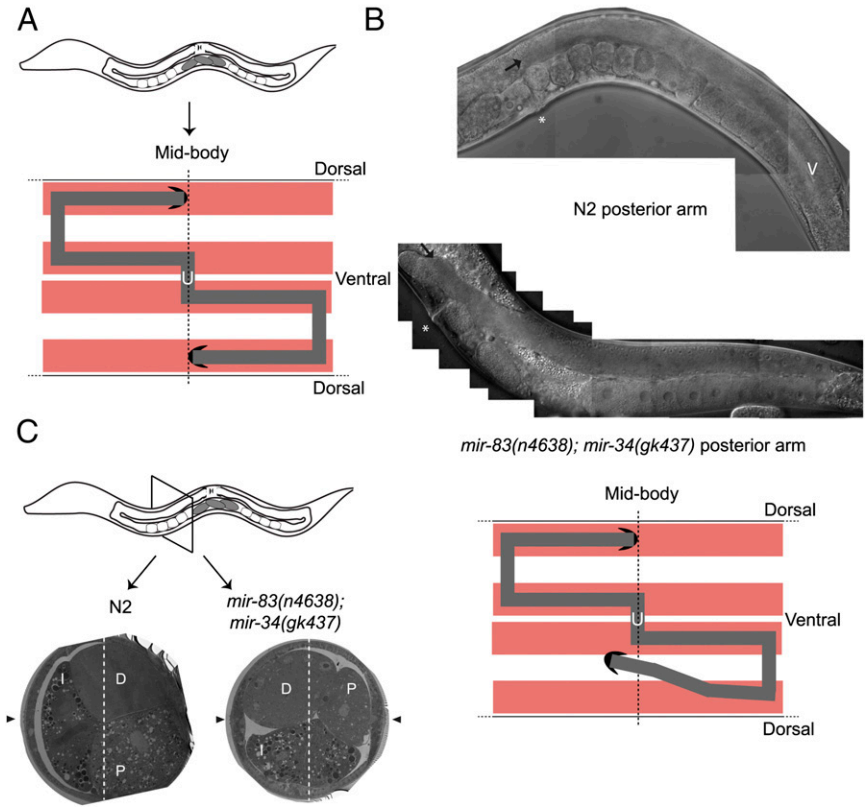

Figure 1 *mir-83(n4638)*; *mir-34(gk437)* mutants have gonad migration defects. (A) The *C. elegans* gonad consists of two *U*-shaped gonad arms. The shape of each arm is created by the migration path of the DTC. The two DTCs are initially located ventrally near the midbody. Each DTC migrates away from the midbody before turning dorsally, migrating to the dorsal body wall muscle, and then migrating back toward the midbody. The path of each DTC can be inferred by the location of the respective gonad arm. Body wall muscle in red, germline in gray, DTCs in black, uterus designated with "U." (B) *mir-83(n4638)*; *mir-34(gk437)* mutants have a gonad migration defect. The improper location of the mature gonad arms implies that DTCs did not migrate along the normal path. In the arm pictured (bottom), the DTC (black arrow) migrated too far, passing the vulva (white asterisk), and is displaced ventrally, as compared to N2 (top). Penetrance quantified in Figure 2. (C) Improper DTC migration causes a rearrangement of internal organs, due to space constraints. In N2 worms, the intestine is positioned laterally with respect to the dorsal/ventral axis (indicated by a white, dashed line), and the proximal and distal segments of the gonad are positioned ventrally and dorsally, respectively, on the other side from the intestine. In the *mir-83(n4638)*; *mir-34(gk437)* worm shown here, the displaced gonad caused a displacement of the intestine. Black arrowheads point to the adult lateral alae, which are positioned on the left and right sides of the animal.

oocyte-containing proximal gonad is located ventrally while the distal gonad is dorsal (Hall and Altun 2008). For a DTC to wander from the appropriate migration path, it must displace the intestine. In addition, the somatic gonad itself will be displaced as it trails behind the migrating DTC. This rearrangement of internal organs, with the intestine, distal gonad arm, and proximal gonad arm all displaced, was visible in both of the two *mir-83(n4638)*; *mir-34(gk437)* mutants sectioned and visualized (Figure 1C).

The penetrance of the migration defect is significantly enhanced by oscillating temperature

We first sought to quantify the penetrance of the migration defect in *mir-83(n4638)*; *mir-34(gk437)* worms raised in standard laboratory conditions, namely on *E. coli*-seeded NGM plates kept at 20° (Brenner 1974). As expected, the DTCs migrate properly in N2 worms in the majority of worms (2 ± 2% migration defective, performed in triplicate, Figure 2A). Both *mir-34(gk437)* and *mir-83(n4638)* single mutant populations display migration defects at a low frequency, 10.67 ± 1.15% and 8 ± 0%, respectively. The phenotype's penetrance is significantly enhanced to 26 ± 7.21% in the *mir-83(n4638)*; *mir-34(gk437)* double mutant ($P \leq 0.05$, unpaired *t*-test), suggesting that the two miRNAs contribute partially redundant functions in the context of DTC migration.

Due to the low penetrance of the phenotype in *mir-83(n4638)*; *mir-34(gk437)* double mutants (Figure 2A), we reasoned that the functions of these miRNAs in DTC migration could be relatively unimportant under standard laboratory conditions, but perhaps more critical under stressful conditions. Therefore, we tested for enhancement of the DTC migration phenotype in worms exposed to various stresses. We observed no change in the penetrance of the phenotype when mutants were exposed continuously throughout development to high temperature (25°) or low temperature (15°) or to a diet of pathogenic *P. aeruginosa*, oxidative stress (0.03% arsenic), or starvation during early larval stages to induce dauer formation (Table S5). However, an enhanced phenotype was observed when worms developed under a changing temperature regimen (Figure 2B), a phenomenon previously observed for *mir-7 Drosophila* mutants in the context of *Drosophila* eye development (Li *et al.* 2009). Semisynchronized populations of developing larvae were exposed to a regimen of temperature changes every 15 min—first from 15° to 25°, and then back to 15°, and so on. The DTC migrations of N2 worms were unaffected by temperature oscillations (0 ± 0%). All three mutant strains [*mir-34(gk437)* and *mir-83(n4638)* single mutants and the *mir-83(n4638)*; *mir-34(gk437)* double mutant] showed an enhanced penetrance of the DTC migration defective phenotype under oscillating temperature compared to constant temperature (20°); from 10.67 ± 1.15% to 28 ± 5.29% for *mir-34(gk437)*, from 8 ± 0% to 16.67 ± 4.16% for *mir-83(n4638)*, and from 26 ± 7.21% to 62.67 ± 4.16% for *mir-83(n4638)*; *mir-34(gk437)*. A similar pattern

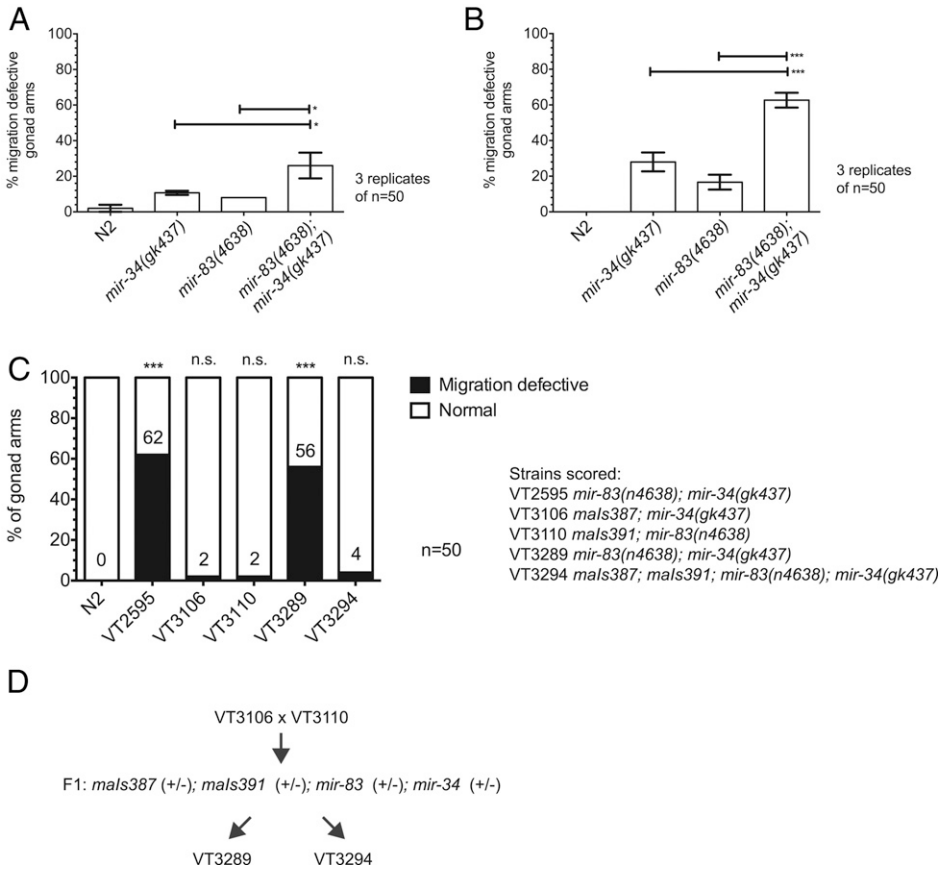

Figure 2 The gonad migration defect is significantly enhanced in *mir-83(n4638); mir-34(gk437)* double mutants. Gonad arm morphology in young adult hermaphrodites was used to score for defects in DTC migrations during larval development at (A) 20° or (B) under an oscillating temperature regimen (15° for 15 min, 25° for 15 min, repeated from plating eggs until young adulthood). (C) Integrated transgenes expressing either *mir-34*, *maIs387* or *mir-83*, *maIs391*, under their natural promoters rescue single mutants. Both VT3289 and VT3294 *maIs387*; *maIs391*; *mir-83(n4638)*; *mir-34(gk437)* were produced by crossing VT3106 *maIs387*; *mir-34(gk437)* to VT3110 *maIs391*; *mir-83 (n4638)*, shown in D. As expected, the newly isolated *mir-83(n4638)*; *mir-34 (gk437)* double mutant, VT3289, displays the migration defect while the double mutant carrying both rescue transgenes, VT3294, appears normal. Significance asterisks compare to N2. Penetrance in VT2595 is not significantly different from penetrance in VT3289. Animals were cycled as described in B. ***P-value $\leq$ 0.005, *0.01 $< P \leq$ 0.05, not significant (n.s.) if $P > 0.05$.

was observed for animals grown on OP50 rather than HB101 *E. coli*, suggesting that the migration defect and its enhancement by oscillating temperature are independent of food source (Figure S2). We also examined a second *mir-34* null allele, *n4276*, and obtained similar results as those for *gk437* (Figure S3).

To confirm that the DTC migration defects of *mir-34* and *mir-83* mutants are a consequence of the loss of the *mir-34* and *mir-83* genes, we generated single-copy integrated rescuing transgenes in their respective single mutant (Table S2). Both the *mir-34* transgene, *maIs387*, and the *mir-83* transgene, *maIs391*, rescue the migration defects of their respective single mutant (Figure 2C). Although this finding supports the conclusion that the migration defects can be explicitly attributed to the *mir-34* and *mir-83* loss of function, a caveat remained that the migration defect was due to background mutations, outside the *mir-34* or *mir-83* loci, that had been present in the single mutants and were segregated away during construction of the transgene-containing strains. In this scenario, the hypothetical background mutations would have been maintained during the construction of the *mir-83(n4638)*; *mir-34(gk437)* double mutant, strain VT2595. To address this caveat, we crossed the *maIs387*; *mir-34(gk437)* and *maIs391*; *mir-83(n4638)* strains together to generate a new doubly mutant *mir-83(n4638)*; *mir-34(gk437)* strain (VT3289) lacking both transgenes and a sibling doubly mutant strain carrying both transgenes (VT3294) (Figure 2C). We observed that VT3289 exhibited a 56% penetrance of migration defective, which is not statistically different from 62% migration defective exhibited by the original *mir-83(n4638)*; *mir-34(gk437)* double mutant, VT2595 (Figure 2C, two-proportion z-test, $P > 0.05$). If the migration defect had been due to background mutations rather than the *mir-34* and *mir-83* deletions we would not expect the newly isolated double to have the defect. As expected, the double mutant carrying both rescue constructs, *maIs387*; *maIs391*; *mir-83(n4638)*; *mir-34(gk437)*, appears mostly normal (4% migration defective).

The above results suggest that DTC migrations may be inherently sensitive to unstable temperature, and that the activity of *mir-34* and *mir-83* helps protect the genetic network controlling this migration from environmental temperature changes. Although the penetrance of the phenotype was increased in *mir-83(n4638)*; *mir-34(gk437)* mutants worms experiencing oscillating temperatures (from 26% at constant 20° to 62.67% in oscillating temperatures), the migration defect is still not fully penetrant in *mir-83(n4638)*; *mir-34(gk437)* mutants, even with temperature oscillations. It was previously shown that for *alg-1* dominant-negative alleles *ma192* and *ma202*, respectively 71% and 73% of worms, have DTC migration defects, strongly suggesting that other miRNAs are involved in the regulation of DTC migrations (Zinovyeva *et al.* 2014). Therefore the additional miRNAs implicated in gonad migration by

the Abbott lab (Brenner *et al.* 2010) were examined to see if being raised in changing temperatures enhanced any of the single mutants as it did for *mir-34(gk437)* and *mir-83(n4638)* mutants. We found that only the *mir-259(n4106)* migration defect appears to be enhanced by oscillating temperatures (Figure 3A), although the enhancement is not significant ($P = 0.086$, two-proportion z-test). Additionally, the migration defects exhibited by *mir-259(n4106)* mutants are similar to those of *mir-34(gk437)* and *mir-83(n4638)* single and double mutants; DTCs improperly cross the dorsal/ventral axis during phase 1 and phase 3 of migration and migrate past the vulva. However, the *mir-259* deletion does not enhance the penetrance of these defects in a triple mutant *mir-83(n4638)*; *mir-259(n4106)*; *mir-34(gk437)* compared to the *mir-83(n4638)*; *mir-34(gk437)* double mutant (Figure 3B, $P \geq 0.05$, two-proportion z-test). This suggests that, although *mir-259* regulates targets involved in DTC migration in a manner that is sensitive to temperature changes and could be involved in the same or a similar process as *mir-34* and *mir-83*, *mir-259* appears to not regulate the same targets as *mir-34* and *mir-83*. If the three miRNAs were acting in parallel on the same set of mRNA targets, we would expect an elevated penetrance of the phenotype upon removal of *mir-259* from the double mutant as the target mRNAs in question would be further derepressed. One caveat regarding this conclusion could be that the lack of enhancement seen in the *mir-83(n4638)*; *mir-259(n4106)*; *mir-34(gk437)* triple compared to the *mir-83(n4638)*; *mir-34(gk437)* double (Figure 3B) might reflect common targets that were fully derepressed in the *mir-83(n4638)*; *mir-34(gk437)* double, such that the loss of an additional regulator had no effect. In this regard, we note that the migration defect penetrance in both the *mir-259(n4106)*; *mir-34(gk437)* and the *mir-83(n4638)*; *mir-259(n4106)* double mutants are weaker than that of the *mir-83(n4638)*; *mir-34(gk437)* mutant (Figure 3C, $P \leq 0.005$, two-proportion z-test). This suggests that the relevant mRNA target sets for *mir-34* and *mir-83* may overlap more with each other than with *mir-259*. For these reasons, we chose to focus on the functionally interacting miRNAs *mir-34* and *mir-83* for the remainder of this study.

The temperature sensitivity of DTC migration is restricted to a 2-hr period during the L1 stage

We next sought to determine if the entire DTC migration process was temperature sensitive in *mir-83(n4638)*; *mir-34(gk437)* mutants, or if there was a more restricted developmental period during which DTCs are sensitive to changing temperature in these mutants. Synchronized populations of N2 and mutant worms were produced by hatching eggs in the absence of food. L1 larvae arrest in such conditions and will not proceed developing until the reintroduction of food (Johnson *et al.* 1984; Baugh 2013). Once food is reintroduced, it takes the larvae ~24 hr at 20° to reach the first molt into the L2 larval stage. Using the DTC-specific reporter, *Plag-2*::GFP (Siegfried and Kimble 2002), we found that the DTCs are born ~16 to 16.5 hr after the reintroduction of food (unpublished results) in both N2 and *mir-83(n4638)*; *mir-34(gk437)* worms. This agrees with previous reports for the timing of DTC birth in N2's (Sulston and Horvitz 1977; Kimble and Hirsh 1979). By examining the effects of 2-hr time windows during which the temperature oscillated between 15° and 25° every 15 min, we found that the temperature-sensitive period for DTCs overlapped with the approximate time of their births. When the 2-hr oscillating temperature regimen occurred before 14 hr of development (Figure 4A) or after 20 hr of development (Figure 4C), *mir-83(n4638)*; *mir-34(gk437)* mutants displayed the migration phenotype at a penetrance similar to that seen in the nonenhanced 20° condition (see Figure 2A). However, when temperature oscillations occurred from hour 16 to hour 18 of development (Figure 4B) we observed an enhanced penetrance of the phenotype similar in magnitude to that of animals that had experienced temperature oscillations throughout larval development (see Figure 2B). This implies that the enhancement observed with temperature oscillations throughout development likely resulted from changing temperature in the interval between hour 16 to hour 18. Indeed, animals that experienced temperature oscillations throughout most of larval development but excluding the 2-hr period from hour 16 to hour 18 did not exhibit phenotypic enhancement (Figure S4).

Our results indicate that cycling between 15° and 25° captures the full enhancement of the migration phenotype under the conditions we have tested. Increasing the upper temperature to 37°, thereby heat shocking the worms in 15-min increments, did not further enhance the penetrance of the phenotype (Figure S5). We also found that the phenotypic enhancement occurred whether the first temperature change was a decrease (Figure 4) or an increase (Figure S6) in temperature and was largely independent of the magnitude of the temperature change; 10-degree or 5-degree changes in temperature resulted in similar phenotype enhancement (Figure S7). We observed that a single oscillation cycle during the hour-16 to hour-18 period was insufficient to enhance the phenotype (Figure S8), suggesting that multiple cycles are necessary to elicit the stress that compromises the integrity of gonad morphogenesis in the absence of *mir-34* and *mir-83*.

Tissue specificity of mir-34 and mir-83

To determine the anatomical site of action of *mir-34* and *mir-83* in regulating the integrity of DTC migrations we generated constructs expressing each of these miRNAs driven by its natural promoter or by promoters from genes expressed in the hypodermis (*dpy-7*), DTCs (*lag-2*, also expressed in some vulval cells), gonadal sheath cells (*lim-7*), or muscle (*myo-3*, also expressed in muscle-like sheath cells 3–5) (Johnstone *et al.* 1992; Henderson *et al.* 1994; Hall *et al.* 1999; Dupuy *et al.* 2007; Fox *et al.* 2007; Ono *et al.* 2007). These constructs were built in Mos1-mediated

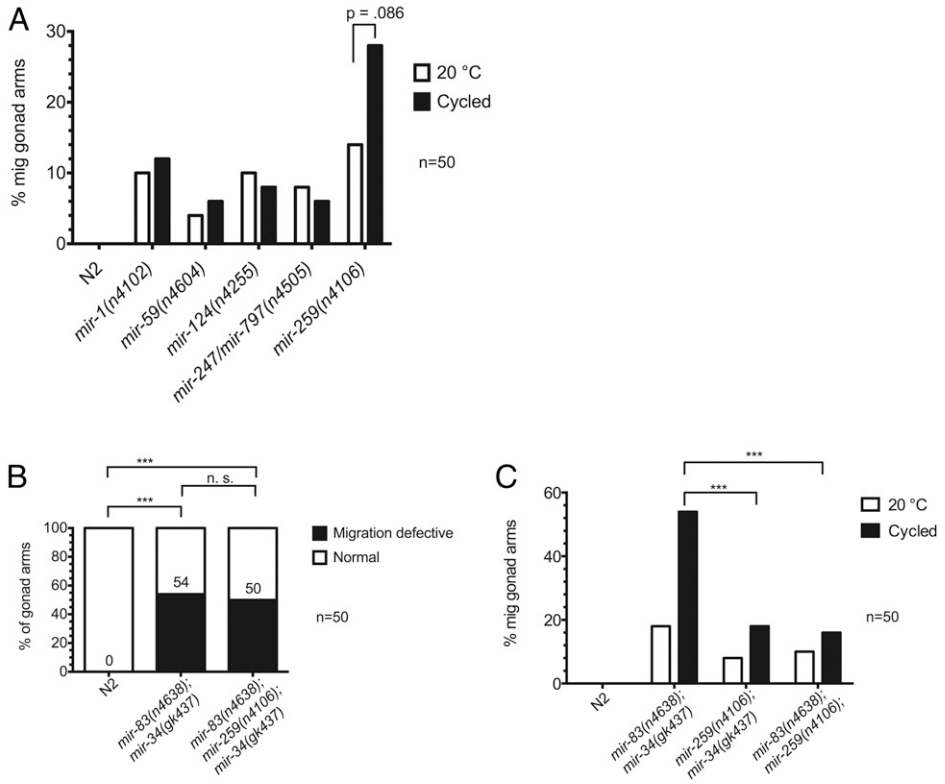

Figure 3 Other miRNAs implicated in gonad migration function in separate pathways. (A) Previously implicated miRNA mutants were tested for enhancement of gonad migration defects by temperature oscillations. Worms were either maintained at a steady 20° throughout development or were subjected to oscillating temperature (15° for 15 min, 25° for 15 min) throughout development ("cycled"). (B) The *mir-259(n4106)* mutation was crossed into the *mir-83(n4638)*; *mir-34(gk437)* strain to assess potential genetic interactions. Worms were subjected to an oscillating temperature regimen (15° for 15 min, 25° for 15 min, repeated until young adulthood). The difference in migration defective (mig) phenotype penetrance between *mir-83(n4638)*; *mir-34(gk437)* and *mir-83(n4638)*; *mir-259(n4106)*; *mir-34 (gk437)* is not significant. ***P-value $\leq$ 0.005. (C) Phenotype penetrance for the *mir-259(n4106)* mutation in combination with either the *mir-34(gk437)* mutation or the *mir-83(n4638)* mutation was compared to that in the *mir-83(n4638)*; *mir-34(gk437)* double mutant. Worms were raised at 20° or cycled during the temperature-sensitive period discussed in Figure 4 [20° for 16 hr (15° for 15 min, 25° for 15 min, repeated three additional times), 20° until young adulthood]. ***P-value $\leq$ 0.005.

single-copy insertion (MosSCI) destination vectors and were used to generate integrated transgenic lines (Frøkjaer-Jensen *et al.* 2008) (Table S2).

As expected, both *mir-34* or *mir-83* expressed under their cognate natural promoters rescued the DTC migration defect of the respective single mutants (Table 1 and Table 2, $P \leq 0.005$, two-proportion z-test). *mir-34(gk437)* and *mir-83(n4638)* phenotypes were also rescued to varying degrees by tissue-specific heterologous promoters. *mir-34* expressed in the DTCs (driven by the *lag-2* promoter; *Plag-2*::*mir-34*) partially rescued the *mir-34(gk437)* defect, from 28.3 to 11.7% (Table 1, $P \leq 0.05$, two-proportion z-test). The lack of full rescue could be due to a difference in expression levels and/or a requirement for *mir-34* in more than one tissue. *mir-83* expressed in either the DTCs (*Plag-2*::*mir-83*) or muscle (*Pmyo-3*::*mir-83*), significantly rescued the migration defect (from 30% in the mutant to 5% in each rescue line, Table 2, $P \leq 0.005$, two-proportion z-test). Potential explanations for this result, where *mir-83* appears to function in either the DTCs or the muscle, are discussed in the *Discussion* section.

Mir-34 and mir-83 regulate two key proteins involved in DTC migrations

Our findings that DTC-specific expression of *mir-34* or *mir-83* can rescue the gonad migration defect of *mir-34(gk437)* or *mir-83(n4638)* mutants suggests that *mir-34* and *mir-83* may regulate a gene or genes whose activity impacts the fidelity of the DTC migration process, and that the migration defect reflects abnormal pathfinding by the DTCs during larval development. An alternative hypothesis, that the displaced gonad arms observed in mutant adults resulted from the shifting of internal organs after otherwise proper migrations, was tested by examining whether the animals' movement impacted their gonad morphology. We observed that the migration-defective phenotype was not affected in genetically paralyzed worms compared to fully active worms, arguing against a contribution of movement-derived structural damage as a cause of the migration defect (Figure S9).

To identify potential targets of *mir-34* and *mir-83* in the regulation of DTC migration, we tested for suppression of the phenotype in *mir-83(n4638)*; *mir-34(gk437)* mutants by RNAi knockdown of genes predicted by mirWIP (Hammell *et al.* 2008) to be targets of both *mir-34* and *mir-83* (Table S1), prioritizing genes known to be involved in cell migrations, larval development, or miRNA function. *cdc-42* and *pat-3*, both expressed in the DTCs and body wall muscle and known to be involved in their migration (Lee *et al.* 2001; Cram *et al.* 2006; Lucanic and Cheng 2008), are predicted targets of *mir-34* and *mir-83* and were subsequently examined.

cdc-42 is a GTPase shown to be downstream of integrin signaling. Upon activation by integrin, *cdc-42* acts to bring about the actin cytoskeleton rearrangements associated with cell migration (Van Aelst and D'Souza-Schorey 1997; Price *et al.* 1998; Ren *et al.* 1999). Previously it has been shown

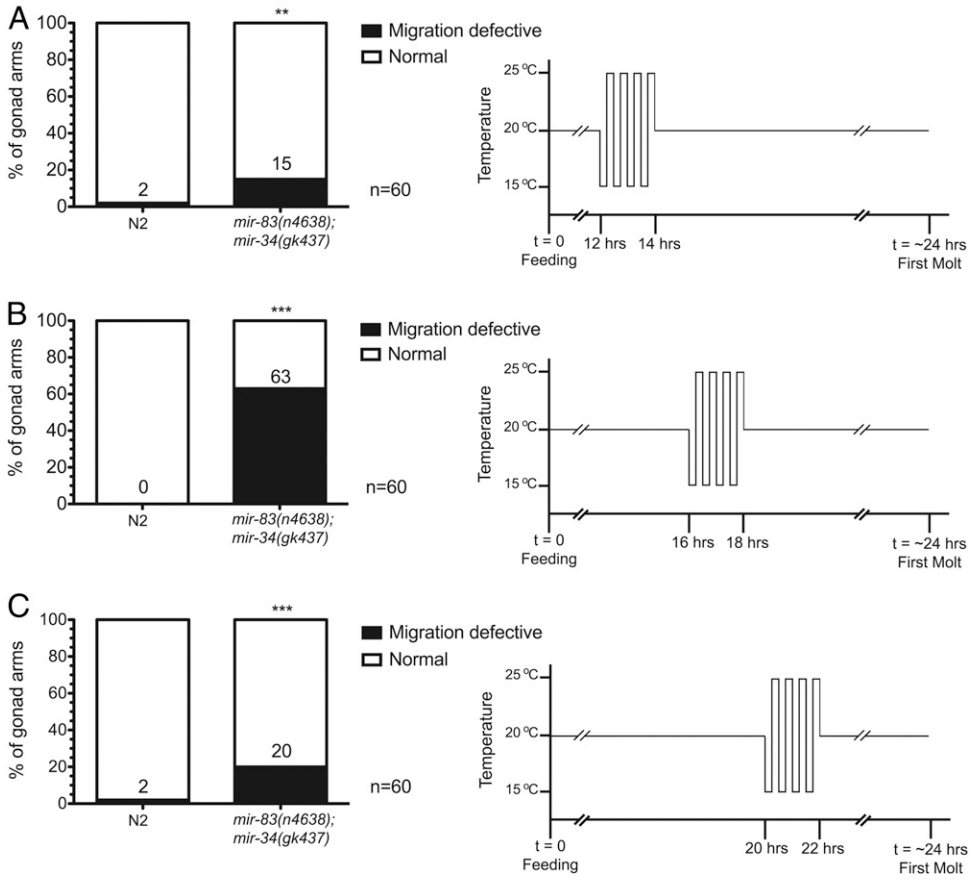

Figure 4 Temperature oscillations within a limited 2-hr window cause the migration defective phenotype enhancement in *mir-83(n4638); mir-34 (gk437)* mutants. The temperature was oscillated every 15 min for a total of 2 hr (15° for 15 min, 25° for 15 min, repeated four times). (A) Temperature oscillations occurred prior to the birth of the DTCs (12 to 14 hr after plating starved L1's on HB101-seeded NGM plates). (B) Temperature oscillations occurred over an interval (16 to 18 hr after plating starved L1's on HB101) corresponding to the time of DTC birth. (C) Temperature oscillations occurred after the birth of the DTCs (20 to 22 hr after plating starved L1's on HB101). ***P-value $\leq$ 0.005, **0.005 $< P \leq$ 0.01, significance asterisks compare N2 to *mir-83(n4638); mir-34(gk437)* mutants.

that when a constitutively active allele of *cdc-42* (unable to hydrolyze GTP to GDP) is expressed in the DTCs, those DTCs display pathfinding defects (Peters *et al.* 2013). If *cdc-42* is a direct target of *mir-34* and *mir-83*, we would expect its expression to be elevated in animals mutant for these two miRNAs. Therefore, we hypothesized that by lowering the level of *cdc-42* in *mir-83(n4638)*; *mir-34(gk437)* mutants we could suppress the gonad migration defect. This is in fact the case. The *cdc-42* null allele *gk388* deletes a portion of *cdc-42*'s 5′ UTR, the first exon, and a portion of the first intron (Kimata *et al.* 2012). *mir-83(n4638)*; *mir-34(gk437)* mutants heterozygous for the *cdc-42(gk388)* allele were significantly rescued, from 53% of the population displaying the gonad migration-defective phenotype to 23% (Figure 5A, $P \leq 0.005$, two-proportion z-test). Mutants containing one copy of *gk388* and wild-type copies of both *mir-34* and *mir-83* also are migration defective (wandering in phase 1 and/or phase 3) at a low penetrance (10% of the population). This is expected as *cdc-42* is a critical regulator of the integrin signaling network (Van Aelst and D'Souza-Schorey 1997; Price *et al.* 1998; Ren *et al.* 1999). We confirmed this suppression using RNAi-induced knockdown of *cdc-42* (Figure 5B); *cdc-42(RNAi)* in a *mir-83(n4638)*; *mir-34(gk437)* mutant significantly suppressed the penetrance of the migration defect from 70 to 37% ($P \leq 0.005$, two-proportion z-test). N2 worms on *cdc-42* RNAi food exhibit wandering phenotypes similar to that observed in the balanced heterozygote. This result supports the idea that the reduction of *cdc-42* is responsible for the suppression seen in *mir-83(n4638)*; *mir-34(gk437)* rather than being the result of the inclusion of the balancer chromosome *mIn1*.

C. elegans has one β-integrin gene, *pat-3* (Williams and Waterston 1994; Gettner *et al.* 1995). Integrin signaling is the major regulatory network involved in phase 1 and phase 3 of DTC migration (Baum and Garriga 1997; Lee *et al.* 2001; Cram *et al.* 2006). Using the *pat-3* null allele *st564* (Williams and Waterston 1994), we created a strain homozygous for deletions of both *mir-34* and *mir-83* and carrying only one functional copy of *pat-3*. In this case, partial loss of *pat*-3 reduced the migration defect from 52 to 25% (Figure 5C, $P \leq 0.005$, two-proportion z-test), supporting the conclusion that *pat-3* overexpression contributes to the migration defect in *mir-83(n4638)*; *mir-34(gk437)* mutants. Note that 18% of worms with one functional copy of *pat-3* are migration defective (we observed wandering during phase 1 and phase 3 and overextension, but no defects in phase 2 turns), indicating that the fidelity of DTC migration may depend critically on *pat-3* dosage. RNAi against *pat-3* also significantly suppressed the migration defect in a *mir-83(n4638)*; *mir-34(gk437)* mutant from 65 to 40% (Figure 5D, $P \leq 0.01$, two-proportion z-test), confirming that the reduction of *pat-3* is responsible for the suppression.

Table 1 Tissue-specific *mir-34* rescue

Strain	Migration defective (%) (*N* = 60)
N2	0
mir-34(gk437)	28.3
Pmir-34::*mir-34*; *mir-34(gk437)*	0***
Pdpy-7::*mir-34*; *mir-34(gk437)*	20
Plag-2::*mir-34*; *mir-34(gk437)*	11.7*
Plim-7::*mir-34*; *mir-34(gk437)*	31.7
Pmyo-3::*mir-34*; *mir-34(gk437)*	26.7

Synchronized L1's were raised with oscillating temperatures: 20° for 16 hr (15° for 15 min, 25° for 15 min, repeated three additional times), 20° until young adulthood. ***P-value ≤ 0.005, *$0.01 < P \leq 0.05$, significance asterisks compare rescue strains to *mir-34(gk437)* mutants.

Table 2 Tissue-specific *mir-83* rescue

Strain	Migration defective (%) (*N* = 60)
N2	0
mir-83(n4638)	30
Pmir-83::*mir-83*; *mir-83(n4638)*	1.7***
Pdpy-7::*mir-83*; *mir-83(n4638)*	25
Plag-2::*mir-83*; *mir-83(n4638)*	5***
Plim-7::*mir-83*; *mir-83(n4638)*	41.7
Pmyo-3::*mir-83*; *mir-83(n4638)*	5***

Synchronized L1's were raised with oscillating temperatures: 20° for 16 hr (15° for 15 min, 25° for 15 min, repeated three additional times), 20° until young adulthood. ***P-value ≤ 0.005, significance asterisks compare rescue strains to *mir-83 (n4638)* mutants.

The suppression in *mir-83(n4638)*; *mir-34(gk437)* mutant phenotype by genetic reduction of either *cdc-42* or *pat-3* activity supports the supposition that *cdc-42* and *pat-3* function downstream of these miRNAs in the regulation of DTC migration. The fact that both *cdc-42* and *pat-3* are predicted to contain sites for both *mir-34* and *mir-83* in their 3′ UTR sequences strongly suggests direct targeting by these miRNAs. In an attempt to gather additional data in support of direct regulation, we constructed a set of nuclear localized mCherry and GFP reporters using the promoters and 3′ UTR sequences of each target (see *Methods*). mCherry was paired with the wild-type target 3′ UTR while GFP was fused to a 3′ UTR where the predicted *mir-34* and *mir-83* binding sites were mutated. Specifically, the 3′ UTR bases predicted to be part of the mRNA–miRNA seed base pairing were mutated to the complementary base, A to T, C to G, G to C, and U to A, such that *mir-34* and *mir-83* loaded miRISCs would no longer to be able to bind the mutated 3′ UTRs. For each wild-type 3′ UTR reporter, the corresponding GFP construct with a mutated 3′ UTR served as an internal control, as it should not be subjected to regulation by either miRNA. The mCherry construct, however, should be regulated by both miRNAs and therefore, should be expressed differently in their presence or absence. We generated multicopy arrays (single-copy transgenes were unsuccessful, see *Discussion*) containing both constructs in *mir-83(n4638)*; *mir-34(gk437)* mutants and crossed these arrays into N2 worms for comparison to the mutant background. GFP and mCherry fluorescence was subsequently quantified within DTCs or for the whole animal. We did not observe a difference in the ratio of mCherry to GFP fluorescence expressed in DTCs for the *cdc-42* reporters, in any of the stages observed (Figure S10A, $P \geq 0.05$, unpaired *t*-test).

As for the *pat-3* reporters, the results were indicative but not definitive. Expression of the *pat-3* reporters was not detectable in DTCs in larval stages. In adults, *pat-3* reporter expression was very dim and bleached rapidly, necessitating scoring whole animals. In whole adult animals, there was a slight increase in the ratio of mCherry to GFP fluorescence for the *pat-3* reporters when *mir-34* and *mir-83* were deleted (Figure S10B, $P \leq 0.05$, unpaired *t*-test), suggesting that the two miRNAs do directly regulate *pat-3*. Although these reporter experiments could not confirm direct regulation of both *cdc-42* and *pat-3* by *mir-34* or *mir-83*, there were numerous technical issues that limited the sensitivity and fidelity of the reporter assays (see *Discussion*). It is possible that *cdc-42* and *pat-3* could be acting in parallel pathways that indirectly oppose the activities of *mir-34* and *mir-83*, such that the observed suppression is the result of decreasing the activity of an opposing pathway. However, based on the computational prediction of cotargeting by *mir-34* and *mir-83*, combined with the fact that both *cdc-42* and *pat-3* are known to be required for proper pathfinding, we propose that these predicted *mir-34* and *mir-83* common targets function downstream of the two miRNAs in conferring robustness to DTC migration in the face of temperature changes.

mir-83(n4638); mir-34(gk437) mutants display reduced cross-progeny fecundity

In addition to guiding the morphology of the adult gonad, DTCs are also required to signal to the germline and regulate the production of germ cells (reviewed in Hubbard and Greenstein 2000). We therefore tested whether the deletion of *mir-34* and *mir-83* affected the function of the hermaphrodite germline by quantifying offspring. We scored the total number of viable progeny, animals that hatched from laid eggs. We did not observe a noticeable difference in the number of dead eggs laid by *mir-83(n4638)*; *mir-34(gk437)* mutants *vs.* N2 worms; therefore, we did not include them in our quantification. When raised at 20° or with temperature oscillations occurring during the previously described 2-hr temperature-sensitive period (referred to as cycled), there was no statistical difference in the number of viable self-progeny produced by *mir-83(n4638)*; *mir-34(gk437)* mutants compared to wild type (Figure 6A, $P \geq 0.05$, unpaired *t*-test).

The self-fertility of a *C. elegans* hermaphrodite is limited by the number of sperm that it produces. Once self-sperm are exhausted, the hermaphrodite's total reproductive capacity is defined by the number of additional oocytes it can produce that are competent to produce viable cross-progeny upon mating to males (Brenner 1974). To investigate cross-progeny production, N2 and *mir-83(n4638)*; *mir-34(gk437)* mutants

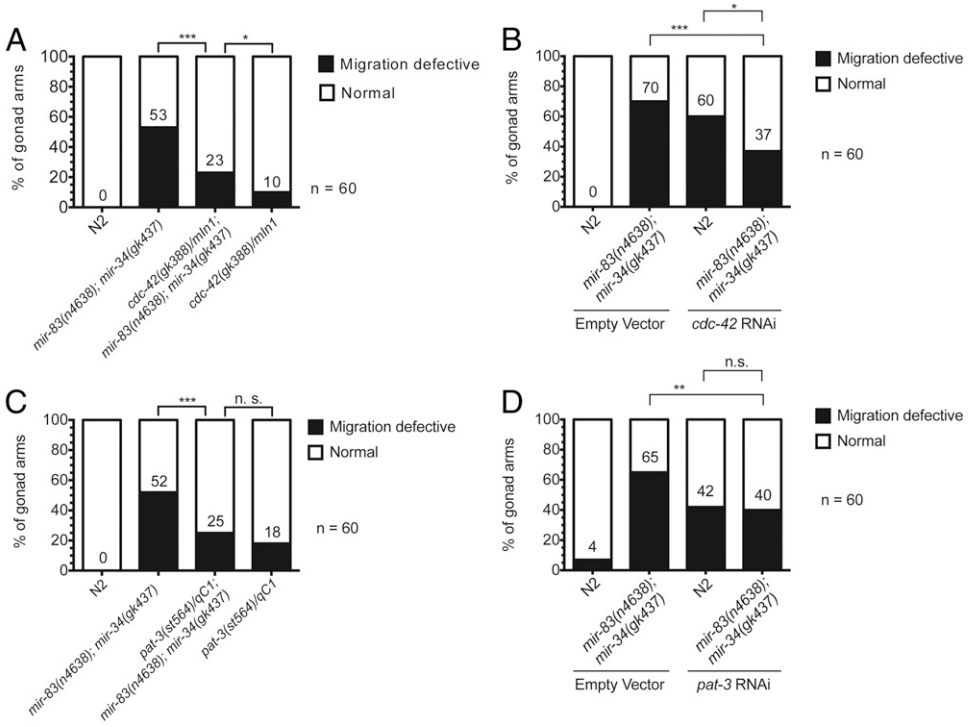

Figure 5 The *mir-83(n4638)*; *mir-34 (gk437)* migration defect is suppressed in *cdc-42* and *pat-3* heterozygotes. The penetrance of the migration defective phenotype is significantly reduced in *mir-83(n4638)*; *mir-34(gk437)* mutants when (A) carrying one copy of *cdc-42*, (B) raised on *cdc-42* RNAi food as compared to empty vector control, (C) carrying one copy of *pat-3*, or (D) raised on *pat-3* RNAi food as compared to empty vector control. Arrested L1's were plated on HB101-seeded NGM plates to restart development. Once plated, temperature was held at 20° for 16 hr, then cycled as follows: 15° for 15 min, 25° for 15 min, four times, then held at 20° until young adulthood. ***P-value $\leq$ 0.005, **0.005 $< P \leq$ 0.01, *0.01 $< P \leq$ 0.05, $P >$ 0.05 not significant (n.s.).

were first either raised at 20° or cycled. After day 4 of adulthood, animals had exhausted their own supply of sperm and could no longer produce fertilized embryos (Byerly *et al.* 1976). At this point, young adult N2 males were mated to aged animals to assess their fertility (Figure 6B). Temperature oscillations did not affect the number of cross-progeny produced by wild-type hermaphrodites crossed to wild-type males (247.25 ± 77.52 *vs.* 236.5 ± 103.44 at 20°, $P \geq 0.05$, unpaired *t*-test). Additionally, there was no significant difference between the number of cross-progeny produced by *mir-83(n4638)*; *mir-34(gk437)* worms raised in either constant temperature or with temperature oscillations when mated to wild-type males (141.85 ± 84.01 at 20° *vs.* 118.65 ± 51.99 cycled, $P \geq 0.05$, unpaired *t*-test). There were, however, significant differences between strains in total cross-progeny produced. Specifically, the number of cross-progeny produced by *mir-83(n4638)*; *mir-34(gk437)* mutants when mated to wild-type males was significantly less than the number of cross-progeny produced by wild-type hermaphrodites mated to wild-type males regardless of the temperature regime during development ($P \leq 0.005$, unpaired *t*-test).

If the fecundity defect in *mir-83(n4638)*; *mir-34(gk437)* hermaphrodites was a direct consequence of the gonad migration defect, we would expect to see a greater number of cross-progeny produced by *mir-83(n4638)*; *mir-34(gk437)* mutants when raised at 20° compared to temperature cycled, as temperature cycling dramatically decreases the percentage of animals with normal gonad morphology. Moreover, we would expect to see two populations of animals within the cycled conditioned, a lower number of viable progeny for the ~60% of the population expected to have a gonad migration defect, and a higher number of viable progeny for the 40% of the population expected to lack any defect. However, the reduced fecundity of *mir-83(n4638)*; *mir-34(gk437)* hermaphrodites was unaffected by temperature regimen and the population distribution of fecundity for *mir-83(n4638)*; *mir-34(gk437)* worms was not consistent with a 60/40% split. Thus it appears that the fecundity defect in *mir-83(n4638)*; *mir-34(gk437)* mutants is likely independent of the gonad migration defect. It is possible that *mir-34* and *mir-83* may regulate targets other than *cdc-42* and *pat-3* within the DTCs that affect their ability to signal to the germline for the regulation of oocyte production. Alternatively, there may be subtle changes in the mating behavior of *mir-83(n4638)*; *mir-34(gk437)* hermaphrodites that could be detected with closer study.

mir-83(n4638); mir-34(gk437) mutants have a decreased lifespan

A rearrangement of internal organs (as seen in Figure 1C) might be expected to have negative consequences for the overall fitness and viability of the affected worm. Moreover, it has been shown that an animal's fecundity can correlate with its longevity (Hsin and Kenyon 1999; Berman and Kenyon 2006; Kenyon 2010). To explore this possibility, we measured the lifespan of N2 and *mir-83(n4638)*; *mir-34(gk437)* mutants raised at either 20° continuously (Figure 7A) or with temperature oscillations during the time-sensitive period (Figure 7B). Although *mir-83(n4638)*; *mir-34(gk437)* worms raised at 20° appeared to have a slightly shortened lifespan compared to N2, the difference was only marginally statistically

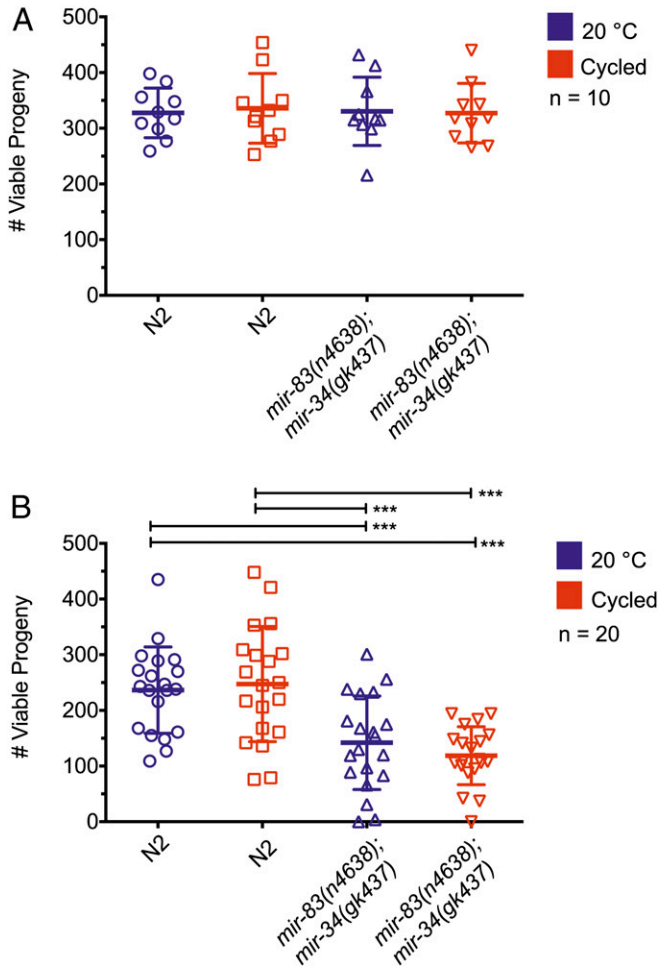

Figure 6 *mir-83(n4638); mir-34(gk437)* mutants produce normal sized self-broods and reduced cross-broods. (A) The total number of living offspring was counted to determine brood size for N2 and *mir-83(n4638); mir-34(gk437)* worms raised at 20° throughout development or subjected to temperature cycles (15° for 15 min, 25° for 15 min, repeated four times) from 16 to 18 hr of development after plating starved L1's on HB101. There is no statistically significant difference between any of the groups. (B) Individual 4-day-old adult hermaphrodites that had exhausted their self-progeny were crossed to four 1-day-old N2 males and number of cross-brood progeny was counted. The average cross-brood size was reduced for *mir-83(n4638); mir-34(gk437)* hermaphrodites whether they were raised at 20° or subjected to temperature cycles (15° for 15 min, 25° for 15 min, repeated four times) from 16 to 18 hr of development. Averages were compared using an unpaired *t*-test, performed by PRISM. ***P-value $\leq$ 0.005. Each group was compared to the three others. The absence of significance asterisks denotes a lack of statistical significance.

significant (Figure 7A, ***$P \leq 0.005$, **$0.005 < P \leq 0.01$, *$0.01 < P \leq 0.05$, unpaired *t*-test). However, for animals subjected to oscillating temperatures during the temperature-sensitive period (from 16 to 18 hr postplating) the difference between N2 and *mir-83(n4638); mir-34(gk437)* mutant worms was more pronounced and statistically significant from day 7 to day 21 (with the exception of days 9 and 17, Figure 7B, ***$P \leq 0.005$, **$0.005 < P \leq 0.01$, *$0.01 < P \leq 0.05$, unpaired *t*-test). The difference in lifespans may be related to the DTC migration phenotype. A relation between the two would explain the slight, less significant difference in lifespan at 20°, when only ~20% of the *mir-83(n4638); mir-34(gk437)* population is migration defective, *vs.* the significant difference in lifespan when animals undergo temperature changes, as now ~60% of the population is migration defective. This hypothesis has yet to be explored as we have not scored individual worms for both the migration phenotype and lifespan due to the fact that scoring for the migration phenotype involves paralyzing the worms and is potentially detrimental to their lifespan. It is possible that the more pronounced difference in lifespan between *mir-83(n4638); mir-34(gk437)* and N2 worms when raised with temperature oscillations does not reflect a direct relationship between lifespan and gonadal migration but instead could reflect a general decrease in the fitness of *mir-83(n4638); mir-34 (gk437)* worms when experiencing temperature changes.

Discussion

There is an obvious benefit for building biological robustness into genetic networks; the fitness of an organism critically depends on the fidelity of developmental processes and reproductive capacity in the face of environmental changes. Previous research across numerous model organisms has described evolutionarily conserved responses to stresses such as food deprivation, heat shock, and various forms of toxicity (reviewed in Lant and Storey 2010). miRNAs are thought to contribute to ensuring the fidelity of gene expression programs in the face of both external stresses and internal transcriptional noise (Li *et al.* 2009) (reviewed in Hornstein and Shomron 2006; Ebert and Sharp 2012; Posadas and Carthew 2014). Previous studies have shown how miRNAs can participate in regulatory loops to precisely regulate gene expression levels (reviewed in Tsang *et al.* 2007; Ebert and Sharp 2012) or establish genetic switches. miRNAs have also been shown to repress leaky transcription, thereby dampening noise within genetic networks (reviewed in Hornstein and Shomron 2006; Posadas and Carthew 2014).

The precise spatiotemporal program of DTC migration is controlled by a complex genetic network including genes *pat-3* and *cdc-42* (Cram *et al.* 2006), which encode, respectively, β-integrin and a GTPase downstream of integrin signaling. Genetic networks need to be robust so as to compensate for adverse changes in gene expression that can result from stress (reviewed in Lant and Storey 2010; Zhou *et al.* 2011). Cells can compensate for stress-induced positive fluctuations in mRNA levels through the post-transcriptional repressive action of miRNAs (Figure 8A). Likewise, negative fluctuations in mRNA levels can be compensated for by activating transcription and/or translation, including releasing inhibition imparted by miRNAs. Thus miRNAs can contribute to the robustness of a genetic network by fine tuning the expression levels of networked genes and

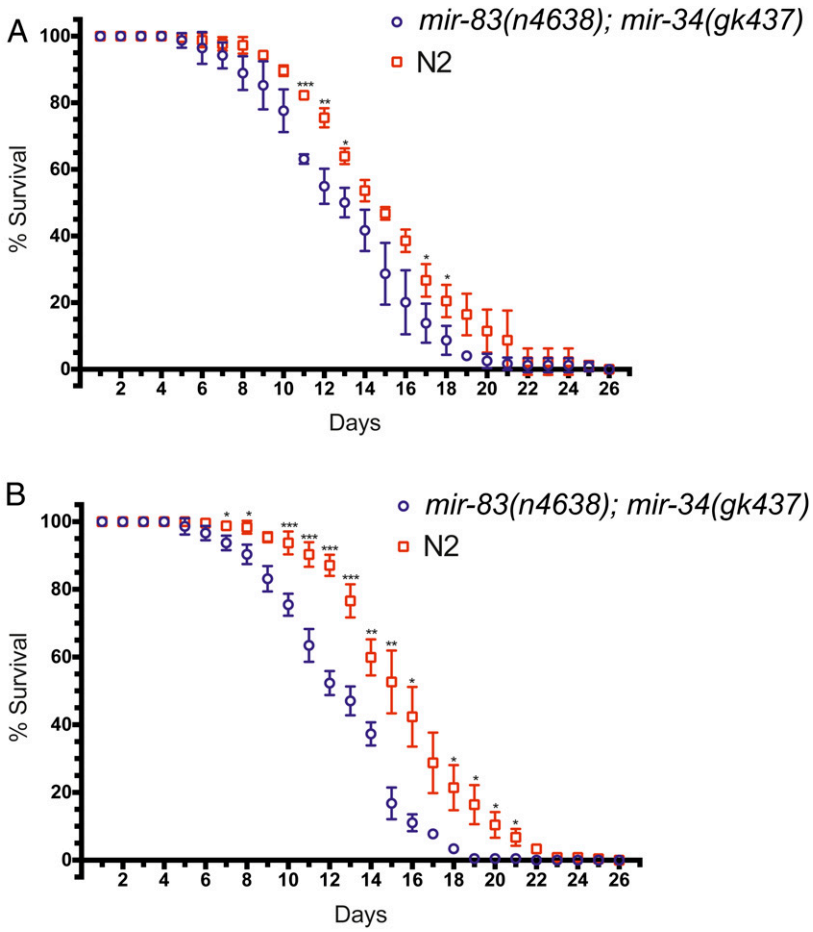

Figure 7 *mir-83(n4638); mir-34(gk437)* mutants have a decreased lifespan compared to wild type. Wild-type (N2) and *mir-83(n4638); mir-34(gk437)* embryos were harvested by hypochlorite treatment and synchronized L1 larvae were obtained by hatching overnight in M9. Larvae were plated on HB101-seeded NGM plates and raised (A) continuously at 20° or (B) subjected to temperature cycles (15° for 15 min, 25° for 15 min, repeated four times) from 16 to 18 hr of development after plating starved L1's on HB101. For each longevity assay shown in panels A and B, 100 animals per replicate, three replicates per condition, were plated as L4's (day 0) and tracked until their death. Alive or dead was determined by prodding worms on their nose and looking for a reaction. Daily averages were compared using a two sample *t*-test for means. ***P-value ≤ 0.005, **$0.005 < P \leq 0.01$, *$0.01 < P \leq 0.05$.

buffering their expression from environmentally driven adverse perturbations.

For DTCs, phase 1 and phase 3 of their migration is regulated by cell-intrinsic integrin signaling (Baum and Garriga 1997; Lee *et al.* 2001; Cram *et al.* 2006; Meighan and Schwarzbauer 2007). We propose that both *mir-34* and *mir-83* help protect the robustness of this genetic network by regulating *cdc-42* and *pat-3* (Figure 8B), particularly when the network is stressed by temperature changes. Our finding that DTC expression of *mir-34* and *mir-83* can rescue the migration defect of their respective mutants supports the hypothesis that the two miRNAs regulate *cdc-42* and *pat-3* within the DTCs. Although these rescue data strongly suggest that *mir-34* and *mir-83* function within the DTCs, we were not able to confirm expression of these miRNAs in DTCs. Transgenes with either the *mir-34* or *mir-83* promoter driving GFP did not produce detectable expression of GFP in the DTCs (although expression in body wall muscle cells was detected for *mir-34* driven GFP). It is possible that the endogenous *mir-34* and *mir-83* genes are expressed in the DTCs, but these transgenic constructs may express GFP at levels below limits of detection.

Interestingly, we also observed rescue of the migration defect in *mir-83(n4638)* mutants by expression of *mir-83* in muscle cells using the *myo-3* promoter. This could reflect a low level of activity of the *myo-3* promoter in the DTCs. Alternatively, it is possible that *mir-83* may perform functions within both the DTCs and muscle, and that function in either cell type can rescue DTC migration. A third possibility is that *mir-83* may function only in the DTCs, but that the *mir-83* miRNA can be supplied either cell intrinsically or cell extrinsically from muscle-expressed *mir-83*. Intriguingly, another known component of the DTC migration gene network, the metalloprotease *mig-17*, is secreted by body wall muscle cells and localizes to the gonadal basement membrane (Nishiwaki *et al.* 2000). It is also possible that *mir-83* synthesized in the muscle could be transported to the DTCs to function, explaining why *mir-83* expression in either of these two tissues can result in similar levels of rescue.

For technical reasons, our fluorescent reporter transgene approach did not permit us to confirm 3′ UTR-dependent regulation of *cdc-42* or *pat-3* by *mir-34* or *mir-83*. Both genes are widely expressed; *cdc-42* is most highly expressed in the intestine and muscles, while *pat-3* expression is particularly high in muscles (unpublished results and Plenefisch *et al.* 2000). Since the two DTCs make up such a small fraction of the worm, protein expression changes within the DTCs are not easily analyzed by Western blotting as expression throughout the entire worm will mask any small cell-specific changes. We used fluorescent reporters due to the difficulty

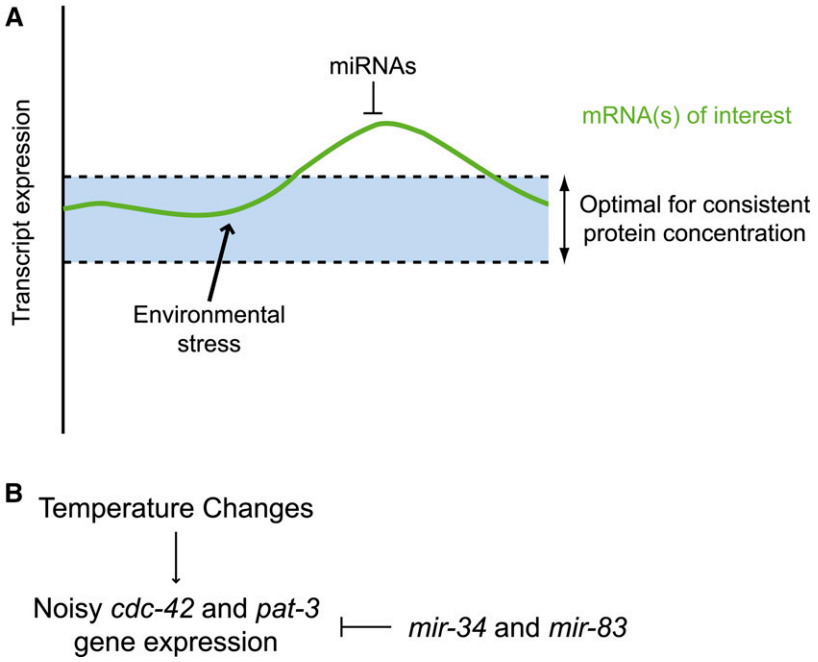

Figure 8 A model proposing robustness functions for *mir-34* and *mir-83* through dampening noisy *cdc-42* and *pat-3* expression in the face of temperature changes. (A) Environmental stresses, such as changing temperatures, may lead to fluctuations in the expression levels of various transcripts, which could challenge cellular proteomic homeostasis. Repression of protein production by miRNAs can provide a means of stabilizing protein output from fluctuating target transcripts. (B) In the case of *mir-34* and *mir-83*, the fidelity of DTC migration is proposed to be maintained in part by inhibiting noisy *cdc-42* and *pat-3* expression incited by unstable environmental temperature.

of seeing cell-specific changes. We first attempted to generate single copy insertions of the four reporters. For both the *pat-3* GFP reporter and the *cdc-42* mCherry reporter, we were not able to generate single copy integrated transgenes that expressed at detectable levels. Therefore we were forced to use multicopy arrays, which most certainly reflect an overexpression of mRNA. We suspect that the absence of measurable response of these reporters to *mir-34* and *mir-83* activity in our experiments likely reflects an overexpression of the reporters, in excess to the endogenous miRNA levels. It is also possible that *mir-34* and *mir-83* may regulate their targets in a fashion too dynamic to visualize using fluorescent reporters.

Here we showed that *mir-34* and *mir-83* both contribute to keeping DTC migrations robust and protecting the fidelity of DTC migratory behavior from changes in temperature. In addition to organizing the morphogenic processes that shape the mature gonad, DTCs are also responsible for regulating meiosis in the germline (Hubbard and Greenstein 2000). Therefore DTCs have a direct impact on *C. elegans* reproductive capacity, and there is a direct benefit for the worm to protect these cells from external stresses. Interestingly, although *mir-83(n4638)*; *mir-34(gk437)* mutants produced the normal number of self-progeny in our experiments, they nevertheless exhibited reduced numbers of cross-progeny when mated to wild-type males. Thus, the overall maximum reproductive capacity of *mir-83(n4638)*; *mir-34(gk437)* hermaphrodites is compromised. Our results suggest that this maximum fecundity defect is not a direct consequence of the gonad migration defect, as the penetrance of the fecundity defect is higher than that of the migration defect and is not enhanced by temperature oscillations. Additionally the fecundity defect may reflect a role for *mir-34* and *mir-83* in regulating fertility that is entirely unrelated to their role in regulating DTC migrations. We do not yet know the pathway or pathways through which *mir-34* and *mir-83* affect fertility or whether the fertility phenotypes represent functions within the germline, DTCs, or both.

We identified a 2-hr temperature-sensitive period, during which temperature oscillations can induce the enhanced DTC migration phenotype of *mir-83(n4638)*; *mir-34(gk437)* hermaphrodites. This temperature-sensitive period overlaps with the birth of the DTCs during the L1 larval stage and is well before the DTCs begin their migration (Sulston 1976; Sulston and Horvitz 1977; Kimble and Hirsh 1979; Sulston *et al.* 1983). We have not determined what aspect of DTC specification and/or differentiation may be inherently sensitive to temperature changes such that in the absence of *mir-34* and *mir-83*, DTCs display a stronger defect in pathfinding fidelity than when under constant temperature. It is intriguing that this defect is enhanced by fluctuating temperature specifically during the L1 stage, suggesting that DTCs are particularly sensitive to the stress of unstable temperature prior to the execution of their migratory program. It is known that the rate of development is closely tied to the environmental temperature in *C. elegans*. Temperature sensitivity during the L1 stage may reflect a requirement to buffer noise within the integrin genetic network early in development. A lack of proper initial buffering may sensitize DTCs such that their subsequent migration is no longer robust. Alternatively, early temperature fluctuations may lead to changes in gene expression that are subsequently buffered by *mir-34* and *mir-83* as the DTCs actively migrate during later larval stages.

In mammals, both *mir-34* and *mir-29* (the mammalian *mir-83* homolog) have been implicated in cancer, and

mir-29 has also been implicated in regulating fibrosis and cell–cell interactions (reviewed in Boominathan 2010; Kriegel *et al.* 2012). Mammalian *mir-34* homologs are transcriptionally activated by p53 and mediate post-transcriptional regulatory processes downstream of p53 (reviewed in He *et al.* 2007; Hermeking 2009; Boominathan 2010). *mir-34a* overexpression has been shown to reduce lung cancer tumor cell proliferation and tumor volume (Xue *et al.* 2014). Human cells contain four paralogs of *mir-29/mir-83*: namely, *mir-29a*, *mir-29b-1*, *mir-29b-2*, and *mir-29c* (reviewed in Kriegel *et al.* 2012). Expression of the *mir-29* miRNAs are regulated by both c-Myc and NF-κB and have been shown to regulate genes involved in apoptosis, cell proliferation, differentiation, and extracellular matrix components (reviewed in Kriegel *et al.* 2012). The *mir-29* miRNAs have been shown to be downregulated in a variety of cancers, including cervical, colon, liver, leukemia, lung, and melanoma (Calin *et al.* 2005; Yanaihara *et al.* 2006; Cummins *et al.* 2006; Pekarsky *et al.* 2006; Garzon *et al.* 2008, 2009; Xiong *et al.* 2010; Li *et al.* 2011; Nguyen *et al.* 2011). They have also been shown to be up-regulated in certain breast cancers. Human CDC42 was shown to be a direct target of the *mir-29* miRNAs in work from the Kim lab (Park *et al.* 2008). Additionally, they showed that the suppression of CDC42 by *mir-29* led to p53 up-regulation and increased apoptosis. Taken together with the work in mammals showing that *mir-34* reinforces p53 negative regulation, this suggests that the coregulation of a genetic network by *mir-34* and *mir-83/mir-29* is evolutionarily ancient and conserved. Furthermore, TargetScan (Lewis *et al.* 2005; Grimson *et al.* 2007; Friedman *et al.* 2009; Garcia *et al.* 2011) predicts conserved targeting of human ITGB1 (integrin beta-1), ITGA11 (integrin alpha-11), and ITGA6 (integrin alpha-6) by the *mir-29* family and conserved targeting for human ITGB8 (integrin beta-8) and ITGA10 (integrin alpha-10) by the *mir-34* family.

Here we show a link between *mir-34*, *mir-83/mir-29*, and integrin-controlled cell migration. Integrin and extracellular matrix misregulation is a key factor in epithelial to mesenchymal transition (EMT) (reviewed in Seguin *et al.* 2015). The implication of *mir-34* and *mir-83/mir-29* in various cancers may reflect a conserved involvement in metastasis through altered EMT that has yet to be explored. The wandering DTC defect in *C. elegans mir-34* and *mir-83/mir-29* mutants, which we have shown results from misregulation of *pat-3* and *cdc-42*, may reflect a homologous miRNA–integrin axis in tumor formation, proliferation, and metastasis in higher animals, including humans.

Acknowledgments

We thank the members of the Ambros lab for helpful discussion, the labs of Nathan Lawson and Oliver Hobert for plasmids, and the lab of Amy Walker for use of their confocal microscope. We also thank the Electron Microscopy Core Facility at the University of Massachusetts for electron microscopy data. The Electron Microscopy Core Facility is supported by award no. S10RR027897 from the National Center For Research Resources. Some strains were provided by the *Caenorhabditis* Genetics Center, which is funded by the National Institutes of Health (NIH) Office of Research Infrastructure Programs (P40 OD010440). The authors are solely responsible for the content of this paper and it does not necessarily represent the official views of the National Center for Research Resources of the NIH. This research was supported by NIH R01GM34028 and by a grant from the Ellison Medical Foundation.

Author contributions: S.L.B. performed the experiments and analyzed the data. S.L.B., M.H., and V.A. designed experiments; S.L.B. and V.A. wrote the paper.

Literature Cited

Alvarez-Saavedra, E., and H. R. Horvitz, 2010 Many families of C. elegans microRNAs are not essential for development or viability. Curr. Biol. 20: 367–373.

Ambros, V., 2004 The functions of animal microRNAs. Nature 431: 350–355.

Ambros, V., R. C. Lee, A. Lavanway, P. T. Williams, and D. Jewell, 2003 MicroRNAs and other tiny endogenous RNAs in *C. elegans*. Curr. Biol. 13: 807–818.

Aravin, A. A., M. Lagos-Quintana, A. Yalcin, M. Zavolan, D. Marks *et al.*, 2003 The small RNA profile during *Drosophila melanogaster* development. Dev. Cell 5: 337–350.

Bartel, D. P., 2004 MicroRNAs: genomics, biogenesis, mechanism, and function. Cell 116: 281–297.

Bartel, D. P., 2009 MicroRNAs: target recognition and regulatory functions. Cell 136: 215–233.

Baugh, L. R., 2013 To grow or not to grow: nutritional control of development during *Caenorhabditis elegans* L1 arrest. Genetics 194: 539–555.

Baugh, L. R., and P. W. Sternberg, 2006 DAF-16/FOXO regulates transcription of cki-1/Cip/Kip and repression of *lin-4* during C. elegans L1 arrest. Curr. Biol. 16: 780–785.

Baum, P. D., and G. Garriga, 1997 Neuronal migrations and axon fasciculation are disrupted in *ina-1* integrin mutants. Neuron 19: 51–62.

Berman, J. R., and C. Kenyon, 2006 Germ-cell loss extends *C. elegans* life span through regulation of DAF-16 by *kri-1* and lipophilic-hormone signaling. Cell 124: 1055–1068.

Boominathan, L., 2010 The guardians of the genome (p53, TA-p73, and TA-p63) are regulators of tumor suppressor miRNAs network. Cancer Metastasis Rev. 29: 613–639.

Brenner, J. L., K. L. Jasiewicz, A. F. Fahley, B. J. Kemp, and A. L. Abbott, 2010 Loss of individual microRNAs causes mutant phenotypes in sensitized genetic backgrounds in *C. elegans*. Curr. Biol. 20: 1321–1325.

Brenner, S., 1974 The genetics of *Caenorhabditis elegans*. Genetics 77: 71–94.

Byerly, L., R. C. Cassada, and R. L. Russell, 1976 *The life cycle of the nematode Caenorhabditis elegans*. I. Wild-type growth and reproduction. Dev. Biol. 51: 23–33.

Calin, G. A., M. Ferracin, A. Cimmino, G. Di Leva, M. Shimizu *et al.*, 2005 A MicroRNA signature associated with prognosis and progression in chronic lymphocytic leukemia. N. Engl. J. Med. 353: 1793–1801.

Cassada, R. C., and R. L. Russell, 1975 The dauer larva, a post-embryonic developmental variant of the nematode *Caenorhabditis elegans*. Dev. Biol. 46: 326–342.

Cram, E. J., H. Shang, and J. E. Schwarzbauer, 2006 A systematic RNA interference screen reveals a cell migration gene network in *C. elegans*. J. Cell Sci. 119: 4811–4818.

Cummins, J. M., Y. He, R. J. Leary, R. Pagliarini, L. A. Diaz *et al.*, 2006 The colorectal microRNAome. Proc. Natl. Acad. Sci. USA 103: 3687–3692.

Dostie, J., Z. Mourelatos, M. Yang, A. Sharma, and G. Dreyfuss, 2003 Numerous microRNPs in neuronal cells containing novel microRNAs. RNA 9: 180–186.

Dupuy, D., N. Bertin, C. A. Hidalgo, K. Venkatesan, D. Tu *et al.*, 2007 Genome-scale analysis of in vivo spatiotemporal promoter activity in *Caenorhabditis elegans*. Nat. Biotechnol. 25: 663–668.

Ebert, M. S., and P. A. Sharp, 2012 Roles for microRNAs in conferring robustness to biological processes. Cell 149: 515–524.

Fox, R. M., J. D. Watson, S. E. Stetina Von, J. McDermott, T. M. Brodigan *et al.*, 2007 The embryonic muscle transcriptome of *Caenorhabditis elegans*. Genome Biol. 8: R188.

Friedman, R. C., K. K.-H. Farh, C. B. Burge, and D. P. Bartel, 2009 Most mammalian mRNAs are conserved targets of microRNAs. Genome Res. 19: 92–105.

Frøkjaer-Jensen, C., M. W. Davis, C. E. Hopkins, B. J. Newman, J. M. Thummel *et al.*, 2008 Single-copy insertion of transgenes in *Caenorhabditis elegans*. Nat. Genet. 40: 1375–1383.

Fukuyama, M., A. E. Rougvie, and J. H. Rothman, 2006 *C. elegans* DAF-18/PTEN mediates nutrient-dependent arrest of cell cycle and growth in the germline. Curr. Biol. 16: 773–779.

Garcia, D. M., D. Baek, C. Shin, G. W. Bell, A. Grimson *et al.*, 2011 Weak seed-pairing stability and high target-site abundance decrease the proficiency of *lsy-6* and other microRNAs. Nat. Struct. Mol. Biol. 18: 1139–1146.

Garzon, R., M. Garofalo, M. P. Martelli, R. Briesewitz, L. Wang *et al.*, 2008 Distinctive microRNA signature of acute myeloid leukemia bearing cytoplasmic mutated nucleophosmin. Proc. Natl. Acad. Sci. USA 105: 3945–3950.

Garzon, R., C. E. A. Heaphy, V. Havelange, M. Fabbri, and S. Volinia *et al*., 2009 MicroRNA 29b functions in acute myeloid leukemia. Blood 114: 5331–5341.

Gettner, S. N., C. Kenyon, and L. F. Reichardt, 1995 Characterization of beta *pat-3* heterodimers, a family of essential integrin receptors in *C. elegans*. J. Cell Biol. 129: 1127–1141.

Grad, Y., J. Aach, G. D. Hayes, B. J. Reinhart, G. M. Church *et al.*, 2003 Computational and experimental identification of *C. elegans* microRNAs. Mol. Cell 11: 1253–1263.

Griffiths-Jones, S., 2004 The microRNA Registry. Nucleic Acids Res. 32: D109–D111.

Griffiths-Jones, S., R. J. Grocock, S. van Dongen, A. Bateman, and A. J. Enright, 2006 miRBase: microRNA sequences, targets and gene nomenclature. Nucleic Acids Res. 34: D140–D144.

Griffiths-Jones, S., H. K. Saini, S. van Dongen, and A. J. Enright, 2008 miRBase: tools for microRNA genomics. Nucleic Acids Res. 36: D154–D158.

Grimson, A., K. K.-H. Farh, W. K. Johnston, P. Garrett-Engele, L. P. Lim *et al.*, 2007 MicroRNA targeting specificity in mammals: determinants beyond seed pairing. Mol. Cell 27: 91–105.

Hall, D. H., and Z. F. Altun, 2008 *C. Elegans Atlas*, Cold Spring Harbor Laboratory Press, Cold Spring Harbor, NY.

Hall, D. H., V. P. Winfrey, G. Blaeuer, L. H. Hoffman, T. Furuta *et al.*, 1999 Ultrastructural features of the adult hermaphrodite gonad of *Caenorhabditis elegans*: relations between the germ line and soma. Dev. Biol. 212: 101–123.

Hammell, M., D. Long, L. Zhang, A. Lee, C. S. Carmack *et al.*, 2008 mirWIP: microRNA target prediction based on microRNA-containing ribonucleoprotein-enriched transcripts. Nat. Methods 5: 813–819.

He, X., L. He, and G. J. Hannon, 2007 The guardian's little helper: microRNAS in the p53 tumor suppressor network. Cancer Res. 67: 11099–11101.

Hedgecock, E. M., J. G. Culotti, D. H. Hall, and B. D. Stern, 1987 Genetics of cell and axon migrations in *Caenorhabditis elegans*. Development 100: 365–382.

Henderson, S. T., D. Gao, E. J. Lambie, and J. Kimble, 1994 *lag-2* may encode a signaling ligand for the GLP-1 and LIN-12 receptors of *C. elegans*. Development 120: 2913–2924.

Hermeking, H., 2009 The *miR-34* family in cancer and apoptosis. Cell Death Differ. 17: 193–199.

Hirsh, D., D. Oppenheim, and M. Klass, 1976 Development of the reproductive system of *Caenorhabditis elegans*. Dev. Biol. 49: 200–219.

Hornstein, E., and N. Shomron, 2006 Canalization of development by microRNAs. Nat. Genet. 38(Suppl): S20–S24.

Houbaviy, H. B., M. F. Murray, and P. A. Sharp, 2003 Embryonic stem cell-specific MicroRNAs. Dev. Cell 5: 351–358.

Hsin, H., and C. Kenyon, 1999 Signals from the reproductive system regulate the lifespan of *C. elegans*. Nature 399: 362–366.

Hubbard, E. J., and D. Greenstein, 2000 The *Caenorhabditis elegans* gonad: a test tube for cell and developmental biology. Dev. Dyn. 218: 2–22.

Irazoqui, J. E., E. R. Troemel, R. L. Feinbaum, L. G. Luhachack, B. O. Cezairliyan *et al.*, 2010 Distinct pathogenesis and host responses during infection of *C. elegans* by *P. aeruginosa* and *S. aureus*. PLoS Pathog. 6: e1000982.

Johnson, T. E., D. H. Mitchell, S. Kline, R. Kemal, and J. Foy, 1984 Arresting development arrests aging in the nematode *Caenorhabditis elegans*. Mech. Ageing Dev. 28: 23–40.

Johnstone, I. L., Y. Shafi, and J. D. Barry, 1992 Molecular analysis of mutations in the *Caenorhabditis elegans* collagen gene *dpy-7*. EMBO J. 11: 3857–3863.

Kamath, R. S., M. Martinez-Campos, P. Zipperlen, A. G. Fraser, and J. Ahringer, 2001 Effectiveness of specific RNA-mediated interference through ingested double-stranded RNA in *Caenorhabditis elegans*. Genome Biol. 2: RESEARCH0002.

Kenyon, C. J., 2010 The genetics of ageing. Nature 464: 504–512.

Kenyon, C., J. Chang, E. Gensch, A. Rudner, and R. Tabtiang, 1993 A *C. elegans* mutant that lives twice as long as wild type. Nature 366: 461–464.

Kimata, T., Y. Tanizawa, Y. Can, S. Ikeda, A. Kuhara *et al.*, 2012 Synaptic polarity depends on phosphatidylinositol signaling regulated by myo-inositol monophosphatase in *Caenorhabditis elegans*. Genetics 191: 509–521.

Kimble, J., and D. Hirsh, 1979 The postembryonic cell lineages of the hermaphrodite and male gonads in *Caenorhabditis elegans*. Dev. Biol. 70: 396–417.

Kimble, J. E., and J. G. White, 1981 On the control of germ cell development in *Caenorhabditis elegans*. Dev. Biol. 81: 208–219.

Kitano, H., 2004 Biological robustness. Nat. Rev. Genet. 5: 826–837.

Kozomara, A., and S. Griffiths-Jones, 2011 miRBase: integrating microRNA annotation and deep-sequencing data. Nucleic Acids Res. 39: D152–D157.

Kozomara, A., and S. Griffiths-Jones, 2014 miRBase: annotating high confidence microRNAs using deep sequencing data. Nucleic Acids Res. 42: D68–D73.

Kriegel, A. J., Y. Liu, Y. Fang, X. Ding, and M. Liang, 2012 The *miR-29* family: genomics, cell biology, and relevance to renal and cardiovascular injury. Physiol. Genomics 44: 237–244.

Lagos-Quintana, M., R. Rauhut, W. Lendeckel, and T. Tuschl, 2001 Identification of novel genes coding for small expressed RNAs. Science 294: 853–858.

Lagos-Quintana, M., R. Rauhut, A. Yalcin, J. Meyer, W. Lendeckel *et al.*, 2002 Identification of tissue-specific microRNAs from mouse. Curr. Biol. 12: 735–739.

Landgraf, P., M. Rusu, R. Sheridan, A. Sewer, N. Iovino *et al.*, 2007 A mammalian microRNA expression atlas based on small RNA library sequencing. Cell 129: 1401–1414.

Lant, B., and K. B. Storey, 2010 An overview of stress response and hypometabolic strategies in *Caenorhabditis elegans*: conserved and contrasting signals with the mammalian system. Int. J. Biol. Sci. 6: 9–50.

Lau, N. C., 2001 An abundant class of tiny RNAs with probable regulatory roles in Caenorhabditis elegans. Science 294: 858–862.

Lee, M., E. J. Cram, B. Shen, and J. E. Schwarzbauer, 2001 Roles for *pat-3* Integrins in Development and Function of *Caenorhabditis elegans* Muscles and Gonads. J. Biol. Chem. 276: 36404–36410.

Lewis, B. P., C. B. Burge, and D. P. Bartel, 2005 Conserved seed pairing, often flanked by adenosines, indicates that thousands of human genes are microRNA targets. Cell 120: 15–20.

Li, X., J. J. Cassidy, C. A. Reinke, S. Fischboeck, and R. W. Carthew, 2009 A microRNA imparts robustness against environmental fluctuation during development. Dev. Cell 137: 273–282.

Li, Y., F. Wang, J. Xu, F. Ye, Y. Shen *et al.*, 2011 Progressive miRNA expression profiles in cervical carcinogenesis and identification of HPV-related target genes for *miR-29*. J. Pathol. 224: 484–495.

Lim, L. P., 2003 The microRNAs of *Caenorhabditis elegans*. Genes Dev. 17: 991–1008.

Lim, L. P., M. E. Glasner, S. Yekta, C. B. Burge, and D. P. Bartel, 2003 Vertebrate microRNA genes. Science 299: 1540.

Liu, Z., S. Kirch, and V. Ambros, 1995 The *Caenorhabditis elegans* heterochronic gene pathway controls stage-specific transcription of collagen genes. Development 121: 2471–2478.

Lucanic, M., and H.-J. Cheng, 2008 A RAC/CDC-42–independent GIT/PIX/PAK signaling pathway mediates cell migration in *C. elegans*. PLoS Genet. 4: e1000269.

Lui, W.-O., N. Pourmand, B. K. Patterson, and A. Fire, 2007 Patterns of known and novel small RNAs in human cervical cancer. Cancer Res. 67: 6031–6043.

Meighan, C. M., and J. E. Schwarzbauer, 2007 Control of *C. elegans* hermaphrodite gonad size and shape by *vab-3*/Pax6-mediated regulation of integrin receptors. Genes Dev. 21: 1615–1620.

Michael, M. Z., S. M. O' Connor, N. G. van Holst Pellekaan, G. P. Young, and R. J. James, 2003 Reduced accumulation of specific microRNAs in colorectal neoplasia. Mol. Cancer Res. 1: 882–891.

Miska, E. A., E. Alvarez-Saavedra, A. L. Abbott, N. C. Lau, A. B. Hellman *et al.*, 2007 Most *Caenorhabditis elegans* microRNAs are individually not essential for development or viability. PLoS Genet. 3: e215–e216.

Mourelatos, Z., J. Dostie, S. Paushkin, A. Sharma, B. Charroux *et al.*, 2002 miRNPs: a novel class of ribonucleoproteins containing numerous microRNAs. Genes Dev. 16: 720–728.

Nguyen, T., C. Kuo, M. B. Nicholl, M.-S. Sim, R. R. Turner *et al.*, 2011 Downregulation of *microRNA-29c* is associated with hypermethylation of tumor-related genes and disease outcome in cutaneous melanoma. Epigenetics 6: 388–394.

Nishiwaki, K., N. Hisamoto, and K. Matsumoto, 2000 A metalloprotease disintegrin that controls cell migration in *Caenorhabditis elegans*. Science 288: 2205–2208.

Ono, K., R. Yu, and S. Ono, 2007 Structural components of the nonstriated contractile apparatuses in the *Caenorhabditis elegans* gonadal myoepithelial sheath and their essential roles for ovulation. Dev. Dyn. 236: 1093–1105.

Park, S.-Y., J. H. Lee, M. Ha, J.-W. Nam, and V. N. Kim, 2008 *miR-29* miRNAs activate p53 by targeting p85α and CDC42. Nat. Struct. Mol. Biol. 16: 23–29.

Pekarsky, Y., U. Santanam, A. Cimmino, A. Palamarchuk, A. Efanov *et al.*, 2006 Tcl1 expression in chronic lymphocytic leukemia is regulated by *miR-29* and *miR-181*. Cancer Res. 66: 11590–11593.

Powell, J. R., and F. M. Ausubel, 2008 Models of *Caenorhabditis elegans* infection by bacterial and fungal pathogens. Methods Mol. Biol. 415: 403–427.

Plenefisch, J. D., X. Zhu, and E. M. Hedgecock, 2000 Fragile skeletal muscle attachments in dystrophic mutants of *Caenorhabditis elegans*: isolation and characterization of the *mua* genes. Development 127: 1197–1207.

Posadas, D. M., and R. W. Carthew, 2014 MicroRNAs and their roles in developmental canalization. Curr. Opin. Genet. Dev. 27: 1–6.

Powell, J. R., and F. M. Ausubel, 2008 Models of *Caenorhabditis elegans* Infection by Bacterial and Fungal Pathogens. Methods Mol. Biol. 415: 403–427.

Poy, M. N., L. Eliasson, J. Krutzfeldt, S. Kuwajima, X. Ma *et al.*, 2004 A pancreatic islet-specific microRNA regulates insulin secretion. Nature 432: 226–230.

Price, L. S., J. Leng, M. A. Schwartz, and G. M. Bokoch, 1998 Activation of Rac and Cdc42 by integrins mediates cell spreading. Mol. Biol. Cell 9: 1863–1871.

Ren, X. D., W. B. Kiosses, and M. A. Schwartz, 1999 Regulation of the small GTP-binding protein Rho by cell adhesion and the cytoskeleton. EMBO J. 18: 578–585.

Rokavec, M., H. Li, L. Jiang, and H. Hermeking, 2014 The p53/*miR-34* axis in development and disease. J. Mol. Cell Biol. 6: 214–230.

Ruaud, A.-F., and J.-L. Bessereau, 2006 Activation of nicotinic receptors uncouples a developmental timer from the molting timer in *C. elegans*. Development 133: 2211–2222.

Sahu, S. N., J. Lewis, I. Patel, S. Bozdag, J. H. Lee *et al.*, 2013 Genomic Analysis of Stress Response against Arsenic in *Caenorhabditis elegans*. PLoS ONE 8: e66431.

Schindler, A. J., L. R. Baugh, and D. R. Sherwood, 2014 Identification of late larval stage developmental checkpoints in *Caenorhabditis elegans* regulated by insulin/IGF and steroid hormone signaling pathways. PLoS Genet. 10: e1004426.

Seguin, L., J. S. Desgrosellier, S. M. Weis, and D. A. Cheresh, 2015 Integrins and cancer: regulators of cancer stemness, metastasis, and drug resistance. Trends Cell Biol. 25: 234–240.

Sempere, L. F., N. S. Sokol, E. B. Dubrovsky, E. M. Berger, and V. Ambros, 2003 Temporal regulation of microRNA expression in *Drosophila melanogaster* mediated by hormonal signals and broad-Complex gene activity. Dev. Biol. 259: 9–18.

Siegfried, K. R., and J. Kimble, 2002 POP-1 controls axis formation during early gonadogenesis in *C. elegans*. Development 129: 443–453.

Stiernagle, T., 2006 Maintenance of C. elegans (February 11, 2006), WormBook, ed. The C. elegans Research Community, WormBook, doi/10.1895/wormbook. 1.101. 1.10.1895/wormbook

Suh, M.-R., Y. Lee, J. Y. Kim, S.-K. Kim, S.-H. Moon *et al.*, 2004 Human embryonic stem cells express a unique set of microRNAs. Dev. Biol. 270: 488–498.

Sulston, J. E., 1976 Post-embryonic development in the ventral cord of *Caenorhabditis elegans*. Philos. Trans. R. Soc. Lond. B Biol. Sci. 275: 287–297.

Sulston, J. E., and H. R. Horvitz, 1977 Post-embryonic cell lineages of the nematode, *Caenorhabditis elegans*. Dev. Biol. 56: 110–156.

Sulston, J. E., E. Schierenberg, J. G. White, and J. N. Thomson, 1983 The embryonic cell lineage of the nematode *Caenorhabditis elegans*. Dev. Biol. 100: 64–119.

Tsang, J., J. Zhu, and A. van Oudenaarden, 2007 MicroRNA-mediated feedback and feedforward loops are recurrent network motifs in mammals. Mol. Cell 26: 753–767.

Van Aelst, L., and C. D'Souza-Schorey, 1997 Rho GTPases and signaling networks. Genes Dev. 11: 2295–2322.

Williams, B. D., and R. H. Waterston, 1994 Genes critical for muscle development and function in *Caenorhabditis elegans* identified through lethal mutations. J. Cell Biol. 124: 475–490.

Wong, M.-C., and J. E. Schwarzbauer, 2012 Gonad morphogenesis and distal tip cell migration in the *Caenorhabditis elegans* hermaphrodite. Wiley Interdiscip. Rev. Dev. Biol. 1: 519–531.

Xiong, Y., J.-H. Fang, J.-P. Yun, J. Yang, Y. Zhang *et al.*, 2010 Effects of *microRNA-29* on apoptosis, tumorigenicity, and prognosis of hepatocellular carcinoma. Hepatology 51: 836–845.

Xue, W., J. E. Dahlman, T. Tammela, O. F. Khan, S. Sood *et al.*, 2014 Small RNA combination therapy for lung cancer. Proc. Natl. Acad. Sci. USA 111: E3553–E3561.

Yamakuchi, M., and C. J. Lowenstein, 2009 *MiR-34*, SIRT1 and p53: the feedback loop. Cell Cycle 8: 712–715.

Yanaihara, N., N. Caplen, E. Bowman, M. Seike, K. Kumamoto *et al.*, 2006 Unique microRNA molecular profiles in lung cancer diagnosis and prognosis. Cancer Cell 9: 189–198.

Zhou, K. I., Z. Pincus, and F. J. Slack, 2011 Longevity and stress in *Caenorhabditis elegans*. Aging (Albany, N.Y. Online) 3: 733–753.

Zinovyeva, A. Y., S. Bouasker, M. J. Simard, C. M. Hammell, and V. Ambros, 2014 Mutations in conserved residues of the *C. elegans* microRNA Argonaute ALG-1 identify separable functions in ALG-1 miRISC loading and target repression. PLoS Genet. 10: e1004286.

Communicating editor: D. I. Greenstein

GENETICS

Supporting Information
www.genetics.org/lookup/suppl/doi:10.1534/genetics.115.179184/-/DC1

Robust Distal Tip Cell Pathfinding in the Face of Temperature Stress Is Ensured by Two Conserved microRNAS in *Caenorhabditis elegans*

Samantha L. Burke, Molly Hammell, and Victor Ambros

DOI: 10.1534/genetics.115.179184

A

C. elegans mir-34	A G G C A G U G U G G U U A G C U G G U U G – –
D. melanogaster mir-34	U G G C A G U G U G G U U A G C U G G U U G U G
M. musculus mir-34a	U G G C A G U G U – C U U A G C U G G U U G U –
M. musculus mir-34b	A G G C A G U G U A A U U A G C U G A U U G U –
M. musculus mir-34c	A G G C A G U G U A G U U A G C U G A U U G C –
H. Sapiens mir-34a	U G G C A G U G U – C U U A G C U G G U U G U –
H. Sapiens mir-34c	A G G C A G U G U A G U U A G C U G A U U G C –

B

C. elegans mir-83	U A G C A C C A U A U A A A U U C A G U A A –
M. musculus mir-29a	U A G C A C C A U C U G A A A U C G G U U A –
M. musculus mir-29b	U A G C A C C A U U U G A A A U C A G U G U U
M. musculus mir-29c	U A G C A C C A U U U G A A A U C G G U U A –
H. Sapiens mir-29a	U A G C A C C A U C U G A A A U C G G U U A –
H. Sapiens mir-29b	U A G C A C C A U U U G A A A U C A G U G U U
H. Sapiens mir-29c	U A G C A C C A U U U G A A A U C G G U U A –

Figure S1 *mir-34* and *mir-83* are highly conserved.
Nucleotide alignments of (A) *mir-34* and (B) *mir-83* sequences. *mir-29* is the mammalian homolog of *mir-83.* Conserved nucleotides are shown in red.

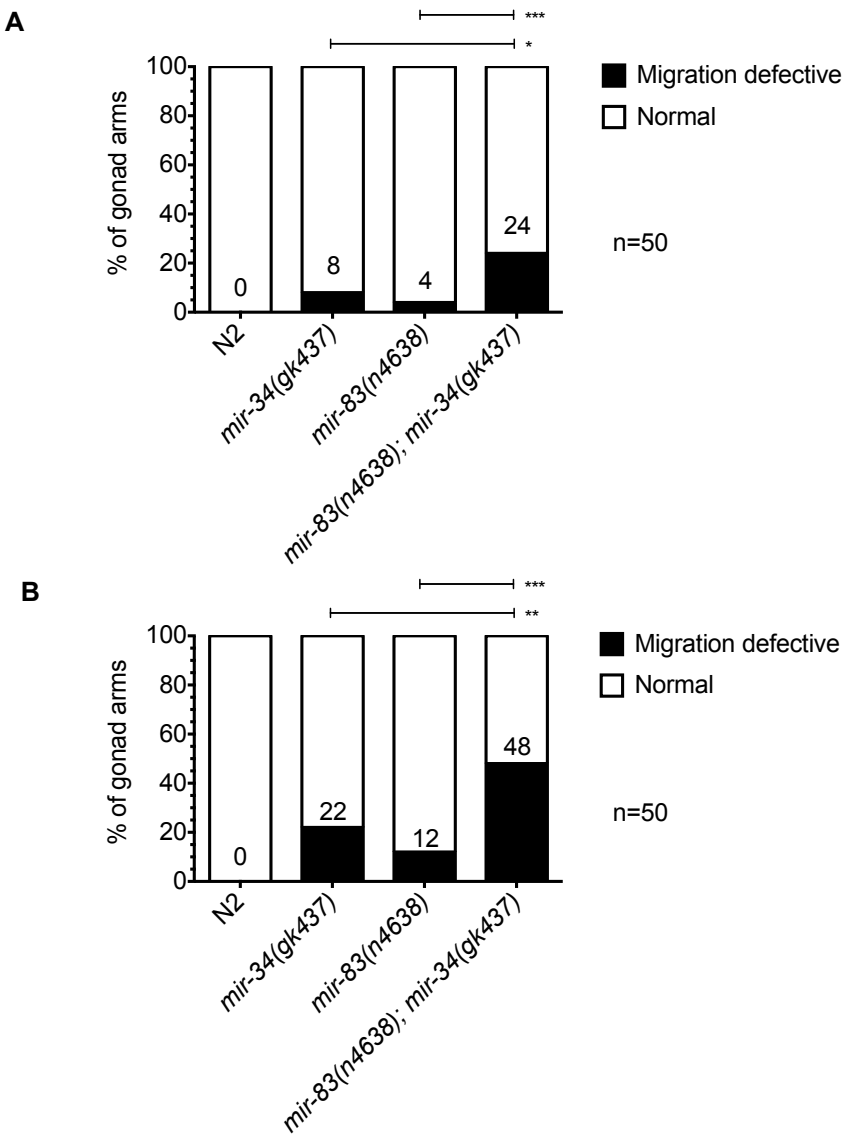

Figure S2 The gonad migration defect is significantly enhanced in *mir-83(n4638); mir-34(gk437)* double mutants raised on OP50 *E. coil*.
(A) Animals raised at 20° or (B) in oscillating temperatures (15° for 15 minutes, 25° for 15 minutes, repeated from plating eggs until young adulthood). *** p-value ≤ .005, ** .005 < p ≤ .01, * .01 < p ≤ .05.

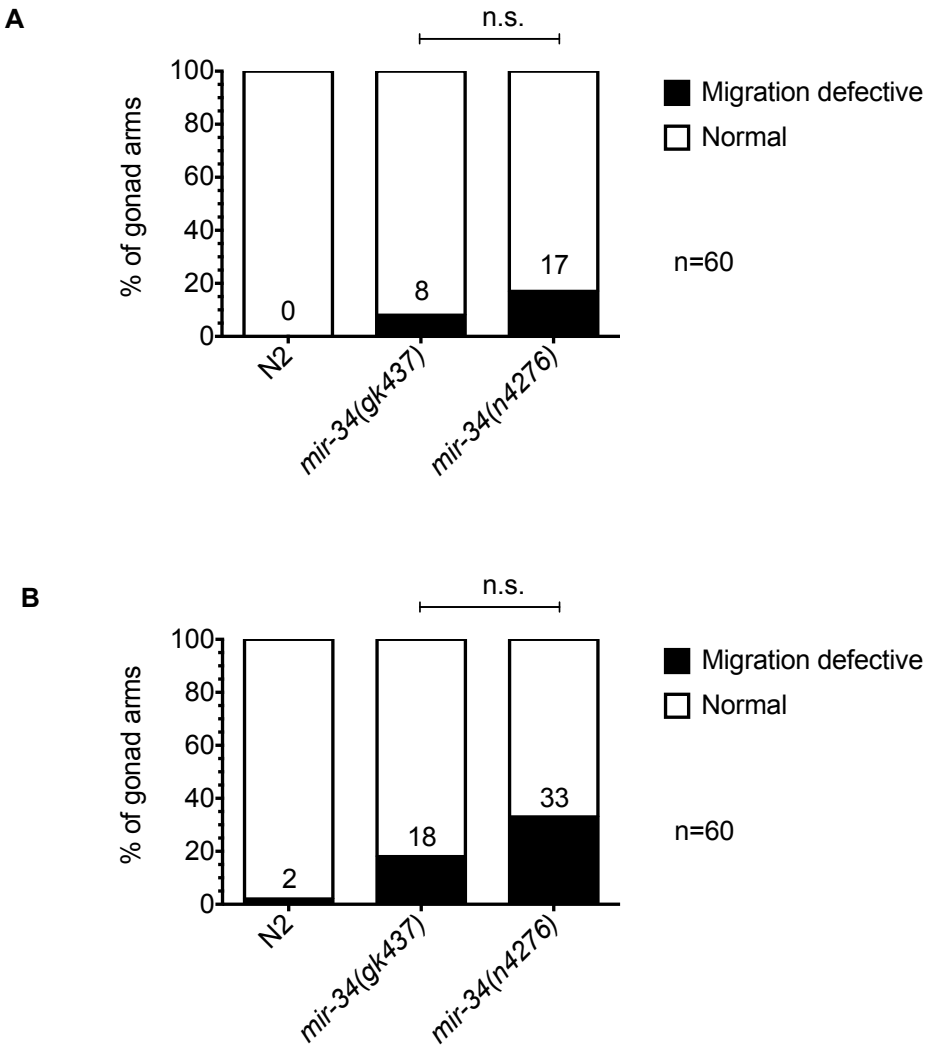

Figure S3 Migration defect seen in two different *mir-34* null alleles.
Animals raised at either (A) 20° or (B) in oscillating temperatures (15° for 15 minutes, 25° for 15 minutes, repeated from plating eggs until young adulthood). Not significant (n.s) if p-value greater than .05.

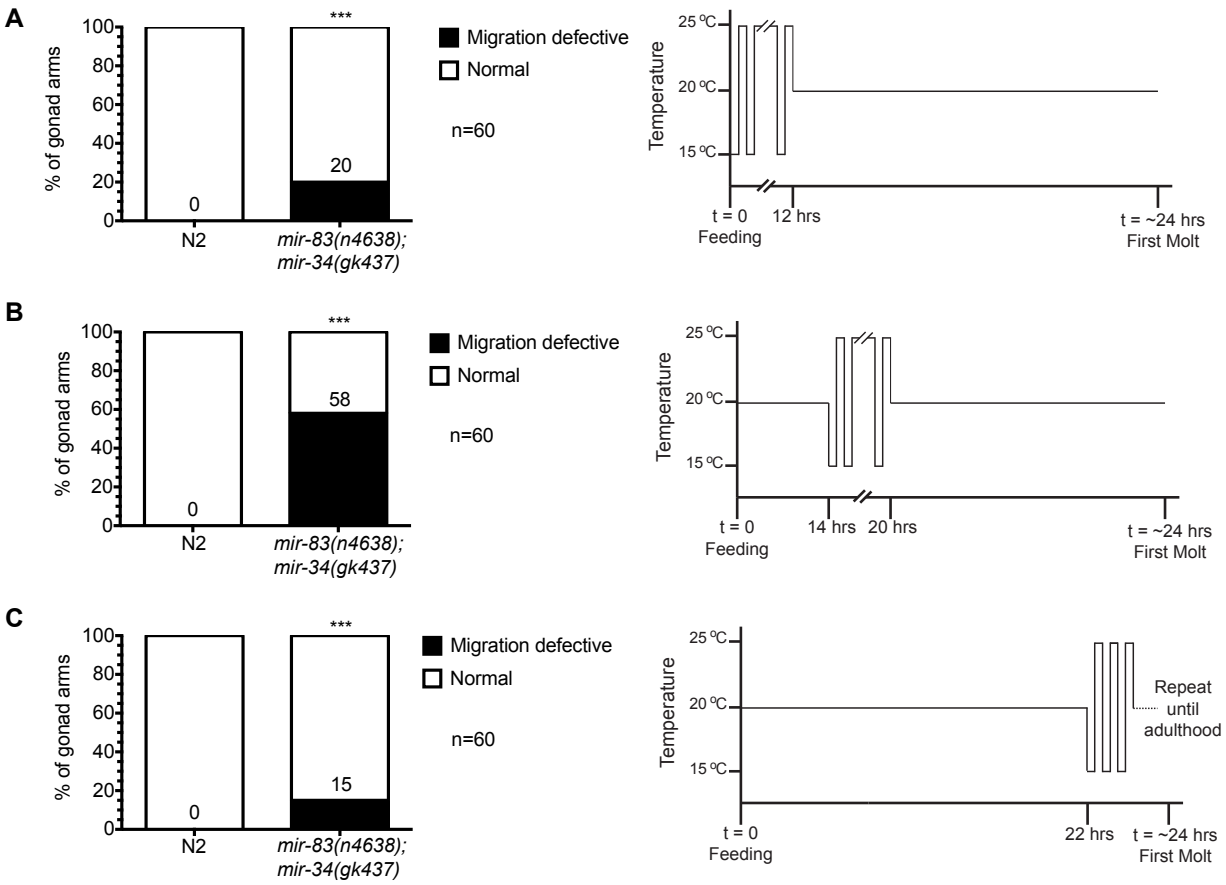

Figure S4 Additional temperature oscillation schemes.
Temperature oscillated between 15º and 25º every 15 minutes for the time windows indicated. (A) For the first 12 hours from the initial plating of starved L1s on HB101-seeded NGM plates. (B) From 14 to 20 hours post-plating L1s, a time period that overlaps with the 2 hour window described in Figure 3. (C) From 22 hours post plating L1s until worms were scored as adults. *** p-value ≤ .005, significance stars compare N2 to *mir-83(n4638); mir-34(gk437)* mutants.

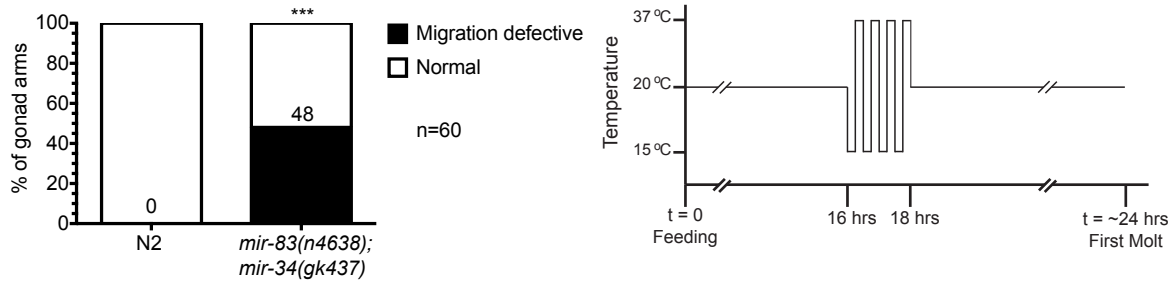

Figure S5 Oscillating temperatures between 15º and 37º does not further enhance the gonad migration defect in *mir-83(n4638); mir-34(gk437)* mutants.
Starved L1s were plated on HB101-seeded NGM plates, grown at 20º for 16 hours, then cycled between 15º and 37º every 15 minutes for a total of 2 hours. *** p-value ≤ .005, significance stars compare N2 to *mir-83(n4638); mir-34(gk437)* mutants.

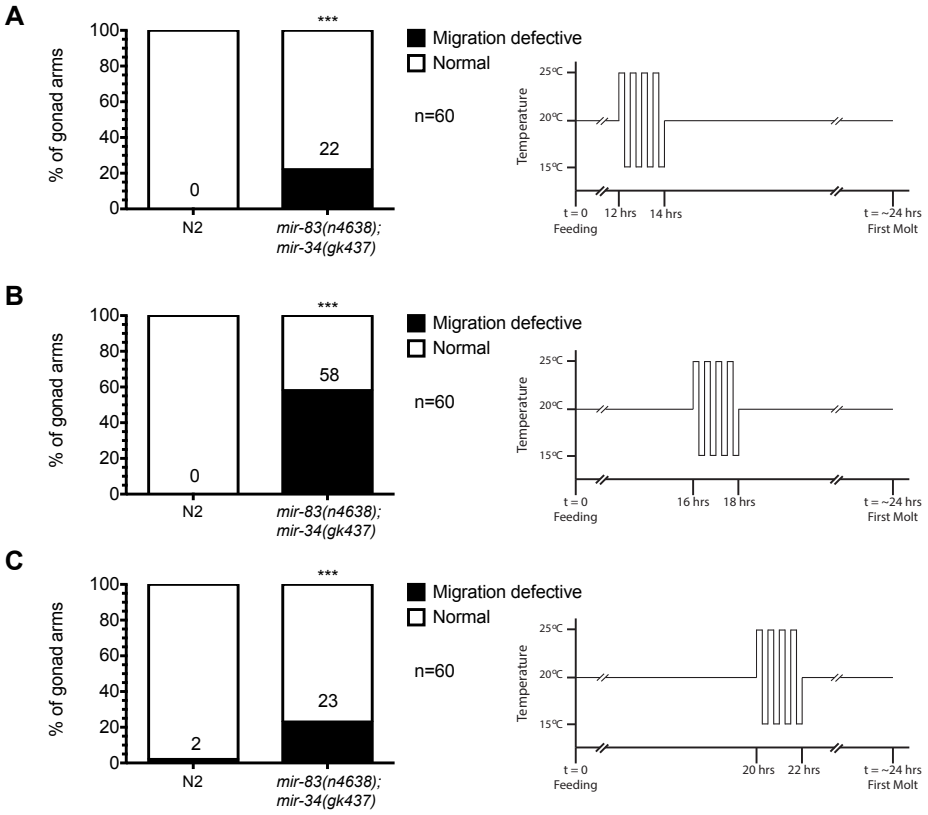

Figure S6 Enhancement of the gonad migration defect is independent of the direction of the initial temperature change. Temperature oscillation schemes were identical to those presented in Figure 3 except the direction of the initial temperature change was reversed. Rather than first lowering the temperature to 15º, the temperature was elevated to 25º for 15 minutes. This was followed by 15 minutes at 15º and repeated three additional times. Oscillations occurred (A) 12-14, (B) 16-18, or (C) 20-22 hours post plating starved L1s. *** p-value ≤ .005, significance stars compare N2 to *mir-83(n4638); mir-34(gk437)* mutants.

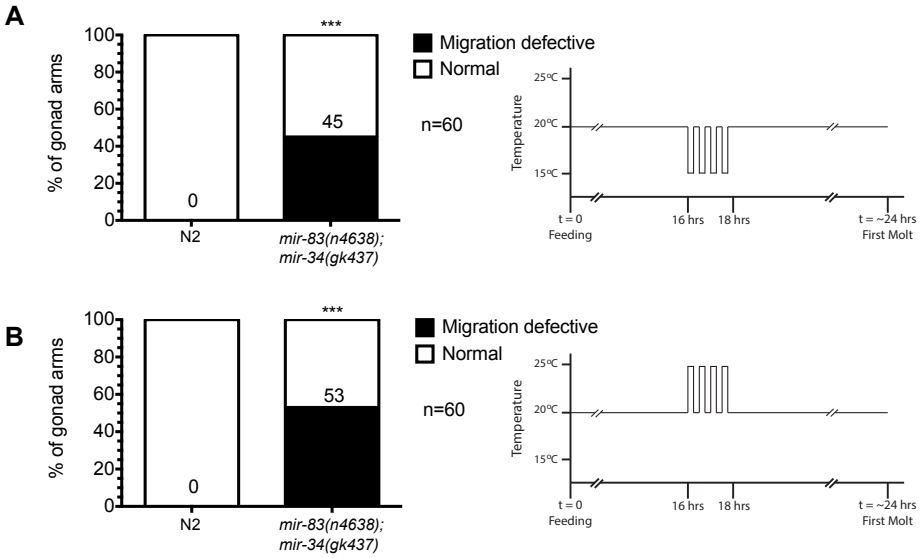

Figure S7 The amount of enhancement of the gonad migration defect is independent of the magnitude of the temperature change.
Five degree changes between (A) 15º and 20º and (B) 20º and 25º during the 2 hour window from 16-18 hours post plating starved L1s. *** p-value ≤ .005, significance stars compare N2 to *mir-83(n4638); mir-34(gk437)* mutants.

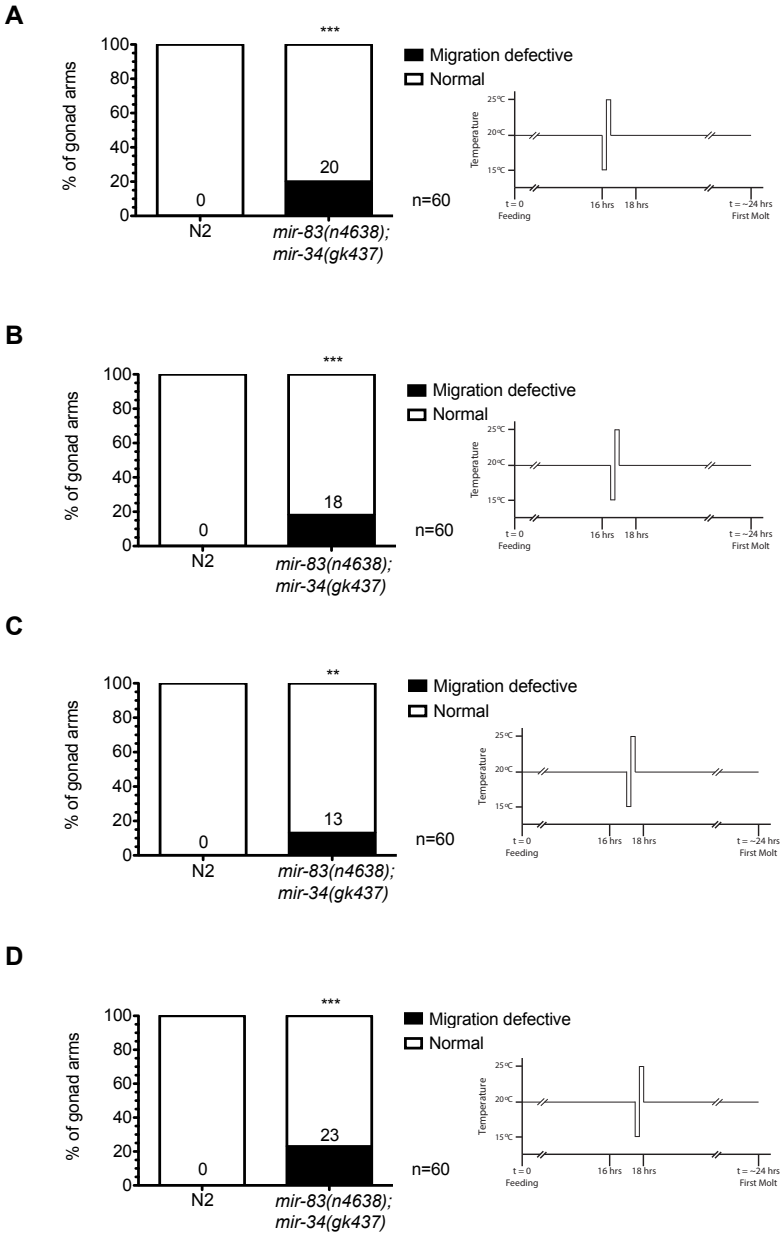

Figure S8 A single temperature cycle is not sufficient to enhance the gonad migration defect in *mir-83(n4638); mir-34(gk437)* mutants.
The 2 hour window consists of four rounds of 15 minutes at 15° followed by 15 minutes at 25°. A single round of temperature cycling is not enough to see an enhancement of the migration phenotype whether that occurs (A) 16 hours, (B) 16.5 hours, (C) 17 hours, or (D) 17.5 hours post plating starved L1s. *** p-value ≤ .005, ** .005 < p ≤ .01, significance stars compare N2 to *mir-83(n4638); mir-34(gk437)* mutants.

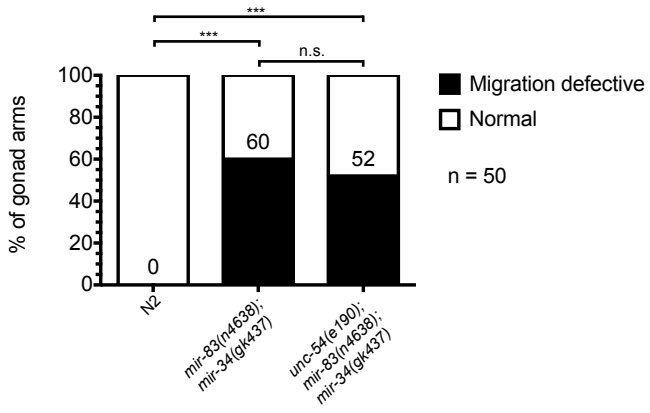

Figure S9 The gonad migration defect in *mir-83(n4638); mir-34(gk437)* mutants is not movement dependent. The *unc-54(e190)* mutation paralyzes worms. The penetrance of the migration defect is not significantly different between *mir-83(n4638); mir-34(gk437)* mutants and *unc-54(e190); mir-83(n4638); mir-34(gk437)* mutants. Starved L1s were plated on HB101-seeded NGM plates, spent 16 hours at 20°, followed by four 15 minutes oscillations between 15° and 25°. *** p-value ≤ .005.

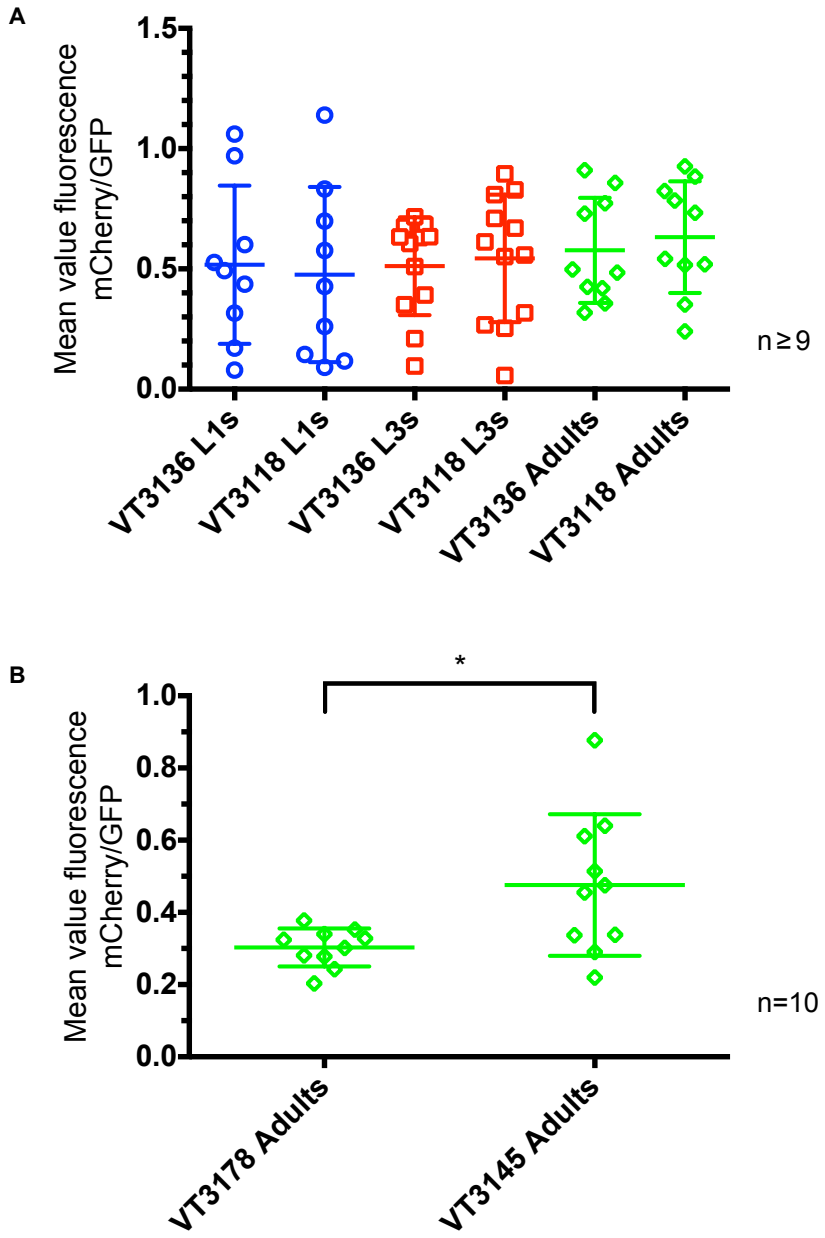

Figure S10 Quantification of *cdc-42* and *pat-3* fluorescent reporters.
Synchronized L1s were plated on HB101-seeded NGM plates and cycled - 20° for 16 hours, [15° for 15 minutes, 25° for 15 minutes, repeated three additional times], 20° until time of scoring. The mean value fluorescence of mCherry was normalized to that of GFP. (A) Ratio of fluorescence within a DTC for worms with *mir-34* and *mir-83* versus the double miRNA mutant (strain VT3136 and VT3118 respectively). (B) Ratio of fluorescence for whole animals for worms with *mir-34* and *mir-83* versus the double miRNA mutant (strain VT3178 and VT3145 respectively). * .01 < p ≤ .05.

Table S1 Predicted targets of both *mir-34* and *mir-83.*

SEQUENCE	GENE NAME	SCREENED
B0348.6	*ife-3*	
C03E10.4	*gly-20*	
C04E6.7		
C06G1.4	*ain-1*	YES
C14F5.5	*sem-5*	YES
C16A3.2		
C16E9.4	*inx-1*	
C23H4.1	*cab-1*	
C26D10.5	*eff-1*	
C34H3.1	*tag-275*	
C38C6.2	*atg-2*	YES
C43H6.6		
C48A7.1	*egl-19*	
C52B9.2	*ets-9*	
C56G2.1	*akap-1*	
D2023.2	*pyc-1*	
F09B9.2	*unc-115*	YES
F14D12.2	*unc-97*	YES
F21A3.3		
F21F8.10	*str-135*	
F39C12.3	*tsp-14*	
F42H10.3		
F46C8.5	*ceh-14*	
F46E10.9	*dpy-11*	
F49E11.1	*mbk-2*	

SEQUENCE	GENE NAME	SCREENED
F53G12.1	*rab-11.1*	
H18N23.2		
H19N07.2	*math-33*	YES
K08B12.5	*tag-59*	YES
K09E9.2	*erv-46*	
M04G12.4	*somi-1*	YES
M106.4	*gmps-1*	
R03G5.1	*eft-4*	
R07B1.9		
R07G3.1	*cdc-42*	YES
R09B5.12	*chil-14*	
R153.1	*pde-4*	
T05A10.1	*sma-9*	
T12G3.1	*sqst-1*	
T14F9.4	*peb-1*	YES
T17H7.4	*gei-16*	
T19A6.1		
T27B1.2	*pat-9*	
T28D9.7	*del-10*	
W01F3.1	*mnr-1*	
W03G9.1	*snf-1*	
W09G10.6	*clec-125*	
Y43H11AL.1		
Y54E10A.9	*vbh-1*	
Y73B6BL.6	*sqd-1*	

SEQUENCE	GENE NAME	SCREENED
ZC64.3	*ceh-18*	YES
ZK1058.2	*pat-3*	YES
ZK112.2	*ncl-1*	
ZK377.2	*sax-3*	YES
ZK994.3	*pxn-1*	

List of genes whose mRNA is predicted to be targeted by both *mir-34* and *mir-83* according to mirWIP. Included are both *cdc-42* and *pat-3*. RNAi was used to knockdown a subset of candidate targets (designated by YES in the SCREENED column) to look for suppression of the migration defect in *mir-83(n4638); mir-34(gk437)* mutants.

Table S2 ***C. elegans*** **Strains**

STRAIN NAME	GENOTYPE
MT12955	*mir-1(n4102)* I
MT12969	*mir-259(n4106)* V
MT15501	*mir-83(n4638)* IV
MT16309	*mir-247 mir-797(n4505)* X
RW3600	*pat-3(st564)/qC1 [dpy-19(e1259) glp-1(q339)]* III
VC898	*cdc-42(gk388)/mIn1 [mIS14 dpy-10(e128)]* II
VT1555	*mir-59(n4604)* IV
VT2392	*mir-34(gk437)* X
VT2527	*mir-124(n4255)* IV
VT2595	*mir-83(n4638)* IV; *mir-34(gk437)* X
VT2797	*pat-3(st564)/qC1 [dpy-19(e1259) glp-1(q339)]* III; *mir-83(n4638)* IV; *mir-34(gk437)* X
VT2812	*unc-54(e190)* I; *mir-83(n4638)* IV; *mir-34(gk437)* X
VT2885	*cdc-42(gk388)/mIn1 [mIS14 dpy-10(e128)]* II; *mir-83(n4638)* IV; *mir-34(gk437)* X
VT2905	*mir-259(n4106)* V; *mir-34(gk437)* X
VT2906	*mir-83(n4638)* IV; *mir-259(n4106)* V; *mir-34(gk437)* X
VT3032	*mir-83(n4638)* IV; *mir-259(n4106)* V
VT3104	*maIs385* [*Plim-7::mir-34 cb unc-119+*] I; *mir-34(gk437)* X
VT3105	*maIs386* [*Pmyo-3::mir-34 cb unc-119+*] I; *mir-34(gk437)* X
VT3106	*maIs387* [*Pmir-34::mir-34 cb unc-119+*] I; *mir-34(gk437)* X
VT3107	*maIs388* [*Plim-7::mir-83 cb unc-119+*] II; *mir-83(n4638)* IV
VT3108	*maIs389* [*Pdpy-7::mir-83 cb unc-119+*] II; *mir-83(n4638)* IV
VT3109	*maIs390* [*Pmyo-3::mir-83 cb unc-119+*] II; *mir-83(n4638)* IV
VT3110	*maIs391* [*Pmir-83::mir-83 cb unc-119+*] II; *mir-83(n4638)* IV
VT3111	*maIs392* [*Plag-2::mir-83 cb unc-119+*] II; *mir-83(n4638)* IV
VT3118	*unc-119(ed3)* III; *mir-83(n4638)* IV; *mir-34(gk437)* X; *maEx246*
VT3123	*maIs396* [*Pdpy-7::mir-34 cb unc-119+*] I; *mir-34(gk437)* X
VT3124	*maIs397* [*Plag-2::mir-34 cb unc-119+*] I; *mir-34(gk437)* X
VT3136	*unc-119(ed3)* III; *maEx246*
VT3145	*unc-119(ed3)* III; *mir-83(n4638)* IV; *mir-34(gk437)* X; *maEx247*
VT3178	*unc-119(ed3)* III; *maEx247*
VT3289	*mir-83(n4638)* IV; *mir-34(gk437)* X
VT3294	*maIs387* I; *maIs391* II; *mir-83(n4638)* IV; *mir-34(gk437)* X

Table S3 Entry vectors and primers

VECTOR	DESCRIPTION	FORWARD PRIMER 5'→ 3'	REVERSE PRIMER 5'→ 3'
pSLB028	*pat-3* 3'UTR	GATAAATAGTTTTTATCCTTATATTTTAAT	CTCGGGGAACAACAACTGACTCTGT
pSLB029	*mir-34* hairpin	CTTAATACCACTACTGACTA	AAGGTTTCTGATCTAAGATG
pSLB032	Mutated *cdc-42* 3'UTR	N/A	N/A
pSLB033	Mutated *pat-3* 3'UTR	N/A	N/A
pSLB035	*cdc-42* promoter	ATATCATATAAACTTGCGAAGGAAT	TTCGCCTGAAAAAAAAAATGAATA
pSLB036	*cdc-42* 3'UTR	GAACGTCTTCCTTGTCTCCATGT	TGTTCCTCTCCTCGTCAAACA
pSLB037	*lim-7* promoter	AGCAATGCTTCCGAAAACC	GCCGTTGAACAGATATAGAAGTTTG
pSLB038	*dpy-7* promoter	AATCTCATTCCACGATTTCT	TTATCTGGAACAAAATGTA
pSLB040	*mir-83* hairpin	TAAAAGCACCACTCGGAACC	AATAGCTCTCGACGCGAAAT
pSLB041	*mir-83* 3' sequence	CTGTATTCAATTATTTGATTC	TTTTCAAGCCAAAACAGAGC
pSLB042	*myo-3* promoter	TGTGTGTGATTGCTTTTTC	TTCTAGATGGATCTAGT
pSLB043	*mir-34* 3' sequence	GAGTTTTTGAAAAGTTGAGG	CACGGCCGCTACCTCCACCTTA
pSLB062	*mir-83* promoter	ACGAATTTCCCACCATTTTG	AATTGAATAATTTGTACCTGCG
pSLB069	*pat-3* promoter	ACGGTATTTTTTCGGGAGA	TTGATGCCGGGTAGGTT
pSLB076	*lag-2* promoter	ACTGGCGCTACTCCACCTT	CTGAAAAAAGGCAAATTTGAAAAG
pSLB080	*mir-34* promoter	N/A	N/A

List of primers used to amplify genomic regions and the resulting Gateway compatible entry vectors created for tissue specific rescue and target sensor constructs.

Table S4 Expression constructs

VECTOR	DESCRIPTION	ENTRY VECTORS	DESTINATION VECTORS
pSLB054	*Pcdc-42::GFP-H2B::*Mutated *cdc-42* 3'UTR	pCM1.35, pSLB033, pSLB035	pCFJ210
pSLB056	*Pcdc-42::mCherry-H2B::cdc-42* 3'UTR	pCM1.151, pSLB035, pSLB036	pCFJ150
pSLB059	*Plim-7::mir-83* hairpin*::mir-83* 3'UTR	pSLB037, pSLB040, pSLB041	pCFJ150
pSLB063	*Pdpy7::mir-83* hairpin*::mir-83* 3' UTR	pSLB038, pSLB040, pSLB041	pCFJ150
pSLB064	*Pmyo-3::mir-83* hairpin*::mir-83* 3' UTR	pSLB040, pSLB041, pSLB042	pCFJ150
pSLB065	*Plim-7::mir-34* hairpin*::mir-34* 3' UTR	pSLB029, pSLB037, pSLB043	pCFJ210
pSLB066	*Pdpy-7::mir-34* hairpin*::mir-34* 3' UTR	pSLB029, pSLB030, pSLB043	pCFJ210
pSLB067	*Pmyo-3::mir-34* hairpin*::mir-34* 3' UTR	pSLB029, pSLB042, pSLB043	pCFJ210
pSLB070	*Pmir-83::mir-83* hairpin*::mir-83* 3'UTR	pSLB040, pSLB041, pSLB062	pCFJ150
pSLB071	*Ppat-3::mCherry-H2B::pat-3* 3'UTR	pCM1.151, pSLB028, pSLB069	pCFJ150
pSLB075	*Ppat-3::GFP-H2B::*Mutated *pat-3* 3'UTR	pCM1.35, pSLB033, pSLB069	pCFJ210
pSLB077	*Plag-2::mir-34* hairpin*::mir-34* 3'UTR	pSLB029, pSLB043, pSLB076	pCFJ210
pSLB078	*Plag-2::mir-83* hairpin*::mir-83* 3'UTR	pSLB040, pSLB041, pSLB076	pCFJ150
pSLB081	*Pmir-34::mir-34* hairpin*::mir-34* 3'UTR	pSLB029, pSLB043, pSLB080	pCFJ210

The noted entry and destination vectors were used to construct the described transgenes for tissue specific rescue and target sensor experiments.

Table S5 Additional stresses

STRESS	STRAIN	MIGRATION DEFECT PENETRANCE
[a]15º	N2	4.5 +/- 6.36%
	mir-34(gk437)	21.5 +/- 12.02%
	mir-83(n4638)	14.5 +/- 0.71%
	mir-83(n4638); mir-34(gk437)	21 +/- 5.66%
[b]25º	N2	5.3 +/- 3.18%
	mir-34(gk437)	13.4 +/- 6.54%
	mir-83(n4638)	11.6 +/- 0.53%
	mir-83(n4638); mir-34(gk437)	24 +/- 5.66%
[c]Arsenic	N2	0% (n=30)
	mir-83(n4638); mir-34(gk437)	27% (n=30)
[d]Dauer	N2	7% (n=60)
	mir-34(gk437)	27% (n=60)
	mir-83(n4638)	25% (n=60)
	mir-83(n4638); mir-34(gk437)	37% (n=60)
[e]*P. aeruginosa*	N2	3% (n=30)
	mir-34(gk437)	13% (n=30)
	mir-83(n4638)	13% (n=30)
	mir-83(n4638); mir-34(gk437)	17% (n=30)

[a]Raised from egg to young adulthood at 15º. Two replicates, n=60 and n=100.
[b]Raised from egg to young adulthood at 25º. Two replicates, n=80 and n=100.
[c]Raised from egg to young adulthood at 20º on NGM plates with 0.03% sodium arsenite.
[d]Dauers isolated from starved plates and moved to fresh plates. Left at 20º until young adulthood.
[e]Raised from egg to young adulthood at 25º on *P. aeruginosa* seeded NGM plates.

Penetrance of the migration defect in the noted strains raised in other stress conditions.